

Eocene to Miocene magnetostratigraphy, biostratigraphy, and chemostratigraphy at ODP Site 1090 (sub-Antarctic South Atlantic)

J.E.T. Channell[†]

Department of Geological Sciences, University of Florida, Post Office Box 112120, Gainesville, Florida 32611, USA

S. Galeotti

Istituto di Geologia, Università degli Studi di Urbino, Campus Scientifico, Località Crocicchia, 61029 Urbino, Italy

E.E. Martin

Department of Geological Sciences, University of Florida, Post Office Box 112120, Gainesville, Florida 32611, USA

K. Billups

College of Marine Studies, University of Delaware, 700 Pilottown Road, Lewes, Delaware 19958, USA

H.D. Scher

Department of Geological Sciences, University of Florida, Post Office Box 112120, Gainesville, Florida 32611, USA

J.S. Stoner

Institute of Arctic and Alpine Research (INSTAAR), University of Colorado, Boulder, Colorado 80309, USA

ABSTRACT

At Ocean Drilling Program (ODP) Site 1090 (lat 42°54.8'S, long 8°54.0'E) located in a water depth of 3702 m on the Agulhas Ridge in the sub-Antarctic South Atlantic, ~300 m of middle Eocene to middle Miocene sediments were recovered with the advanced piston corer (APC) and the extended core barrel (XCB). U-channel samples from the 70–230 meters composite depth (mcd) interval provide a magnetic polarity stratigraphy that is extended to 380 mcd by shipboard whole-core and discrete sample data. The magnetostratigraphy can be interpreted by the fit of the polarity-zone pattern to the geomagnetic polarity time scale (GPTS) augmented by isotope data and bioevents with documented correlation to the GPTS. Three normal-polarity subchrons (C5Dr.1n, C7Ar.1n, and C13r.1n), not included in the standard GPTS, are recorded at Site 1090. The base of the sampled section is correlated to C19n (middle Eocene), although the interpretation is unclear beyond C17r. The top of the sampled section is correlated to C5Cn (late early Miocene), although, in the uppermost 10 m

of the sampled section, a foraminifer (*Globorotalia sphericomiozea*) usually associated with the Messinian and early Pliocene has been identified. ⁸⁷Sr/⁸⁶Sr, $\delta^{13}\text{C}$, and $\delta^{18}\text{O}$ values measured on foraminifera, including the $\delta^{18}\text{O}$ and $\delta^{13}\text{C}$ shifts close to the Eocene/Oligocene boundary, support the correlation to the GPTS. For the interval spanning the Oligocene/Miocene boundary, benthic $\delta^{13}\text{C}$, $\delta^{18}\text{O}$, and ⁸⁷Sr/⁸⁶Sr records from Site 1090 can be correlated to isotope records from ODP Site 929 (Ceara Rise), providing support for the recently-published Oligocene/Miocene boundary age (22.92 Ma) of Shackleton et al.

Keywords: Cenozoic, magnetostratigraphy, stable isotopes, strontium isotopes, biostratigraphy, South Atlantic.

INTRODUCTION

Ocean Drilling Program (ODP) Site 1090 (lat 42°54.8'S, long 8°54.0'E) is located on the flank of the Agulhas Ridge (subantarctic South Atlantic) in a water depth of 3702 m (Fig. 1). Drilling at this site began on Christmas Day, 1997. The pre-cruise objective at Site 1090 was to recover an upper Miocene–Pleistocene section at moderate resolution to

study past migrations of the Polar Front and monitor the influence of North Atlantic Deepwater and Circumpolar Deepwater in this part of the Southern Ocean. Unexpectedly, a hiatus was encountered at 70 mcd (meters composite depth) that accounted for the absence of the lower Pliocene–middle Miocene section (Shipboard Scientific Party, 1999). Beneath the hiatus, an ~310 m section of lower Miocene–middle Eocene mainly pale reddish-brown nannofossil and diatom oozes was recovered with the use of the Advanced Piston Corer (APC) and Extended Core Barrel (XCB). Magnetic susceptibility, bulk density using the gamma-ray attenuation porosity evaluator (GRAPE), and color reflectance were the bases for the shipboard determination of depth offsets in the composite section (Shipboard Scientific Party, 1999). It was determined that the cores from three holes (1090B, 1090D, and 1090E) provide continuous overlap to at least 212 mcd and possibly to 245 mcd.

The bulk of the ~310 m section studied (70–380 mcd) consists of lithologic unit II (70–352 mcd): pale reddish-brown mud-bearing diatom ooze and diatom-bearing nannofossil ooze, with carbonate varying in the 0–80% range (Shipboard Scientific Party, 1999). Magnetic susceptibility values for unit

[†]E-mail: jetc@ufl.edu.

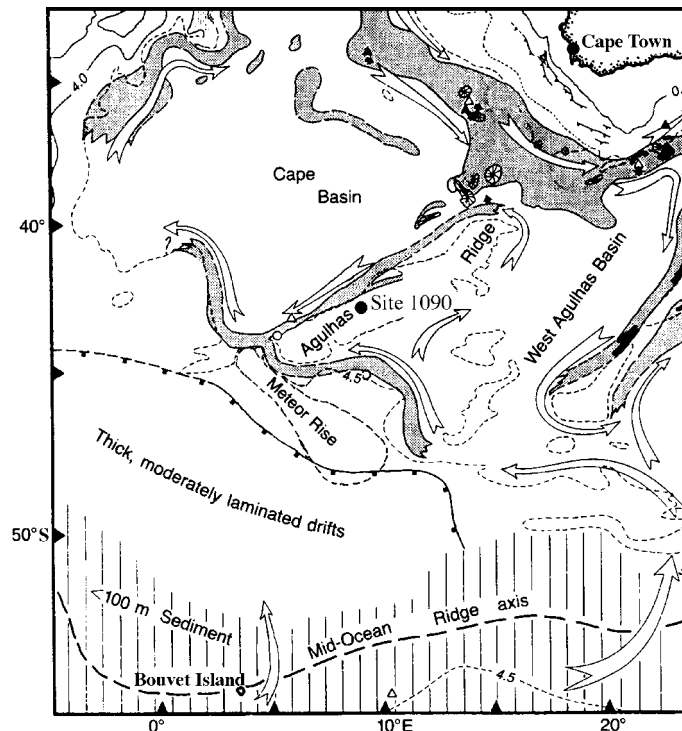


Figure 1. Location of ODP Site 1090. Shading indicates circumbasin erosional zone separating Cape Basin and West Agulhas Basin (after Tucholke and Embley, 1984; Ciesielski et al., 1988; Gersonde et al., 1999).

II are higher than for the overlying pale gray nannofossil ooze of unit I (0–70 mcd), where carbonate percentages are generally in the 70%–80% range (Shipboard Scientific Party, 1999). Unit III (>352 mcd) comprises brown mud-bearing nannofossil ooze with very variable carbonate content.

Here we document the magnetic polarity stratigraphy for the Eocene–Miocene section from three types of samples. (1) Archive halves of core sections from three holes measured by using the shipboard pass-through magnetometer, (2) discrete (7 cm³) samples collected from Hole 1090B measured postcruise, and (3) u-channel samples, having a 2 × 2 cm square cross-section and a length up to 1.5, collected from the composite section, also measured postcruise. Interpretation of the magnetostratigraphy is aided by ⁸⁷Sr/⁸⁶Sr, $\delta^{13}\text{C}$, and $\delta^{18}\text{O}$ values measured on planktic and benthic foraminifera.

The magnetic polarity stratigraphy spans the interval between polarity chrons C19n (middle Eocene) and C5Cn (late early Miocene). This ~26 m.y. (ca. 41–15 Ma) interval is represented by 310 m of section, represented by 310 m of section, having an average sedimentation rate of 12.4 m/m.y. The thickness, time span, and quality of the paleomagnetic record makes it comparable with the

classic Cenozoic magnetostratigraphic records recovered by deep-sea drilling, such as Deep Sea Drilling Project (DSDP) Hole 608 for the Miocene (Clement and Robinson, 1987) and DSDP Site 522 for the Oligocene (Tauxe et al., 1983, 1984). On land, the Contessa section near Gubbio (Italy) spans the Eocene and Oligocene and provides a “type section” for the magnetostratigraphy of this time interval (Lowrie et al., 1982). The mean sedimentation rate for the Eocene–Miocene section at ODP Site 1090 is comparable to the Miocene sedimentation rate at DSDP Site 608 and is approximately twice the mean sedimentation rates at DSDP Site 522 and in the Contessa section. The higher-resolution record at Site 1090 reveals several polarity subchrons not recorded in sections with lower mean sedimentation rates.

MAGNETIC MEASUREMENTS

The natural remanent magnetization (NRM) of archive halves of core sections from Holes 1090B, 1090D, and 1090E were initially measured by using the shipboard pass-through magnetometer. Progressive stepwise demagnetization and measurement were carried out at four steps up to a maximum peak field of 20 mT. Further shipboard demagnetization would

have compromised the sediments for additional (u-channel) studies. Discrete (7 cm³) samples in plastic containers were collected from the working halves of cores from Hole 1090B at a spacing of ~1–2 per 150-cm-long core section. Postcruise, about half the discrete samples were stepwise demagnetized in 14 steps up to a peak field of 80 mT. The other half of the discrete samples was thermally demagnetized in 16 steps (100–640 °C) until remanence fell below magnetometer noise level. U-channel samples, with a 2 × 2 cm cross section and length up to 1.5 m, were collected from the archive halves of the composite section. U-channel samples were demagnetized and measured in 12 steps using peak fields from 20 to 100 mT by using the 2G Enterprises pass-through magnetometer at the University of Florida (see Weeks et al., 1993).

Alternating field (AF) demagnetization of the discrete samples and u-channel samples indicated that the NRM occasionally survived peak alternating fields of 80–100 mT, indicating the presence of high-coercivity remanence carriers (Fig. 2A). In order to investigate the blocking-temperature spectrum of the NRM through thermal demagnetization, discrete samples were measured, removed from their plastic containers, wrapped in aluminum foil, and remeasured. The wrapped samples were then thermally demagnetized in temperature increments up to 640 °C (Fig. 2B). A large proportion of the magnetization is lost at 575 °C; however, in some cases a small proportion of the NRM has unblocking temperatures above the Curie point (maximum blocking temperature) of magnetite. From the AF and thermal demagnetization data, we infer that the NRM is carried by magnetite with a minor contribution from hematite for some samples. In Figure 2, the three projections showing AF demagnetization data from u-channel samples (collected from the archive halves of the core section) are from the same depth as the thermal demagnetization data from discrete samples (collected from the working halves of core sections). The component declinations differ by 180° for u-channel and discrete sample data, reflecting the sampling of archive and working halves, respectively.

The inclination data after demagnetization at peak fields of 20 mT from the shipboard magnetometer for Holes 1090B, 1090D, and 1090E are shown together with component inclinations from discrete samples in the left-side column of Figures 3A and 3B and in Figure 4. For the discrete samples, the demagnetization range in which the characteristic magnetization component is isolated was picked by eye from orthogonal projections,

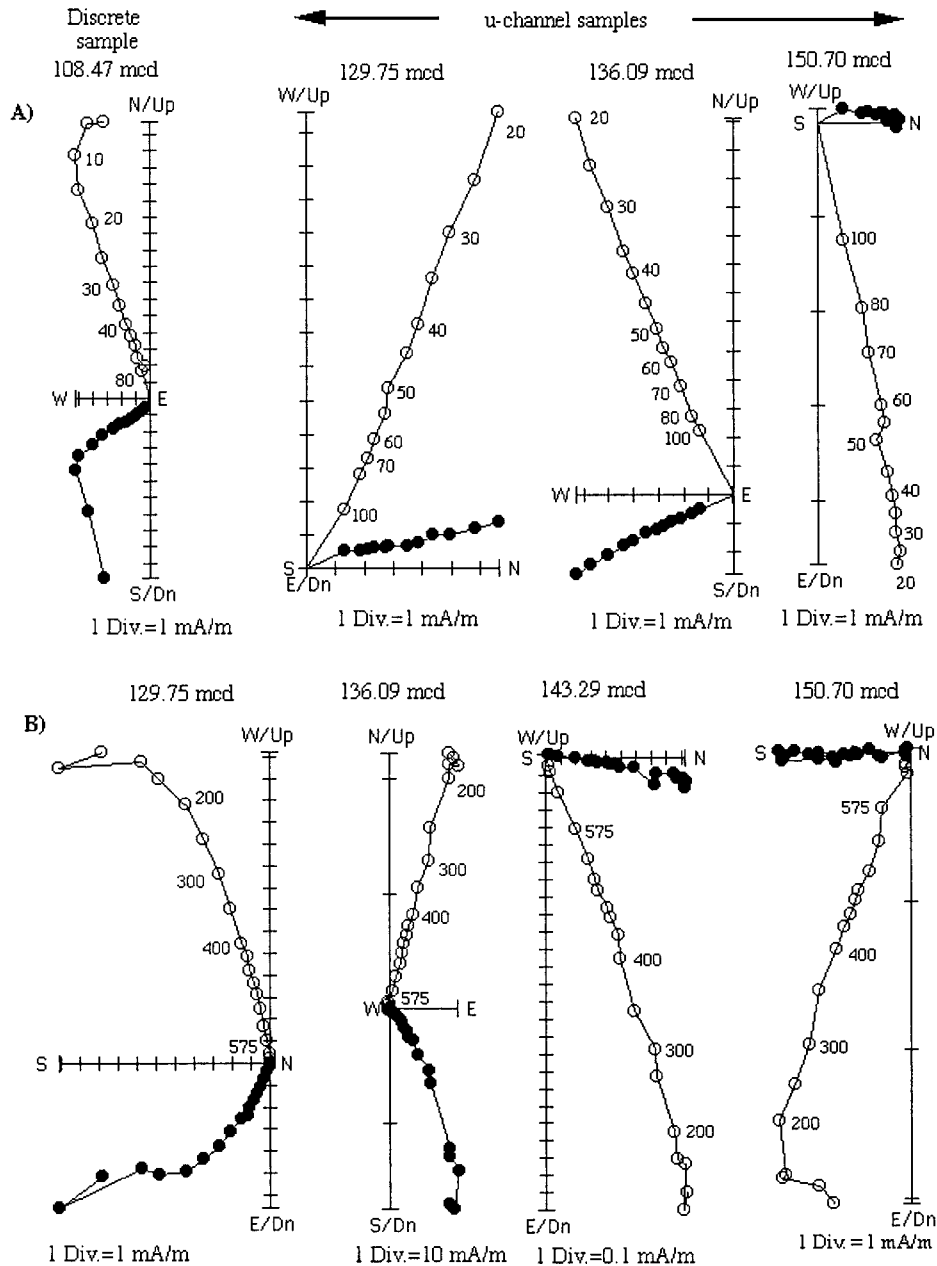


Figure 2. (A) Orthogonal projection of alternating field demagnetization data for one discrete sample from Hole 1090B and for levels in the u-channels collected from the composite section. Peak alternating fields are indicated in milliteslas. (B) Orthogonal projection of thermal demagnetization data for four discrete samples from Hole 1090B. Temperatures are indicated in degrees Celsius. The initial point represents the NRM of the sample in its plastic case, and the second point represents the NRM after removal from the plastic case and wrapping in Al foil. Open and closed symbols indicate projection of vector endpoints on the vertical and horizontal planes, respectively. The magnetization intensity associated with one division on the axes of each plot is indicated. Note that u-channel levels in (A) have been picked to coincide with some of the thermally demagnetized samples in (B). Declinations are $\sim 180^\circ$ apart for discrete and u-channel samples as they were collected from the working and archive halves of core sections, respectively.

and component inclinations were calculated by using the standard least-squares method (Kirschvink, 1980). Discrete samples (from Hole 1090B) are consistent with Hole 1090B shipboard data; however, in some intervals, such as the 105–110 mcd interval, the Hole 1090B data are discrepant with respect to data from Holes 1090E and 1090D (Fig. 3A). This finding is attributed to imprecision in shipboard hole-to-hole correlation. As the u-channel record was derived from the composite section, and the composite section in this interval was constructed entirely from Holes 1090E and 1090D, the u-channel record is not affected by the mismatch with Hole 1090B.

The u-channel record (Figs. 3A, 3B) comprises component declinations and inclinations calculated at 1 cm intervals by using the standard least-squares method (Kirschvink, 1980) to calculate the magnetization components for the 20–80 mT demagnetization range. The maximum angular deviation (MAD) values are less than 20° for all data plotted in Figure 3A and 3B, indicating that the magnetization components are reasonably well defined. In the 70–167 mcd interval, the composite section jumps numerous times between Holes 1090D and 1090E (Shipboard Scientific Party, 1999). Hole 1090B, as well as Holes 1090D and 1090E, are utilized from 167 mcd to the base of the composite section at 240 mcd. At each tie-point where the composite section jumps from one hole to another, there is a short overlap in u-channel sampling. A mismatch of up to 50 cm at the 125.71 mcd level is attributed to imprecise hole-to-hole correlation between Holes 1090D and 1090E at this level (Fig. 3A). U-channel sampling was discontinued at 228 mcd, close to the base of the APC section, where the stiffness of the sediment precluded further u-channel sampling. Below this level, we utilize shipboard pass-through magnetometer data, and component magnetization directions from 7 cm³ discrete samples (Fig. 4). The discrete sample component directions, based on thermal and alternating field demagnetization, are generally consistent with the shipboard pass-through data. Below ~ 347 mcd, drilling disturbance in the XCB section has resulted in a poorly defined magnetostratigraphy (Fig. 4).

INTERPRETATION OF MAGNETOSTRATIGRAPHY

The interpretation of the magnetostratigraphy can be accomplished by fitting the polarity-zone pattern to polarity chrons in the GPTS of Cande and Kent (1992), aided by isotope stratigraphy and biostratigraphy (Fig.

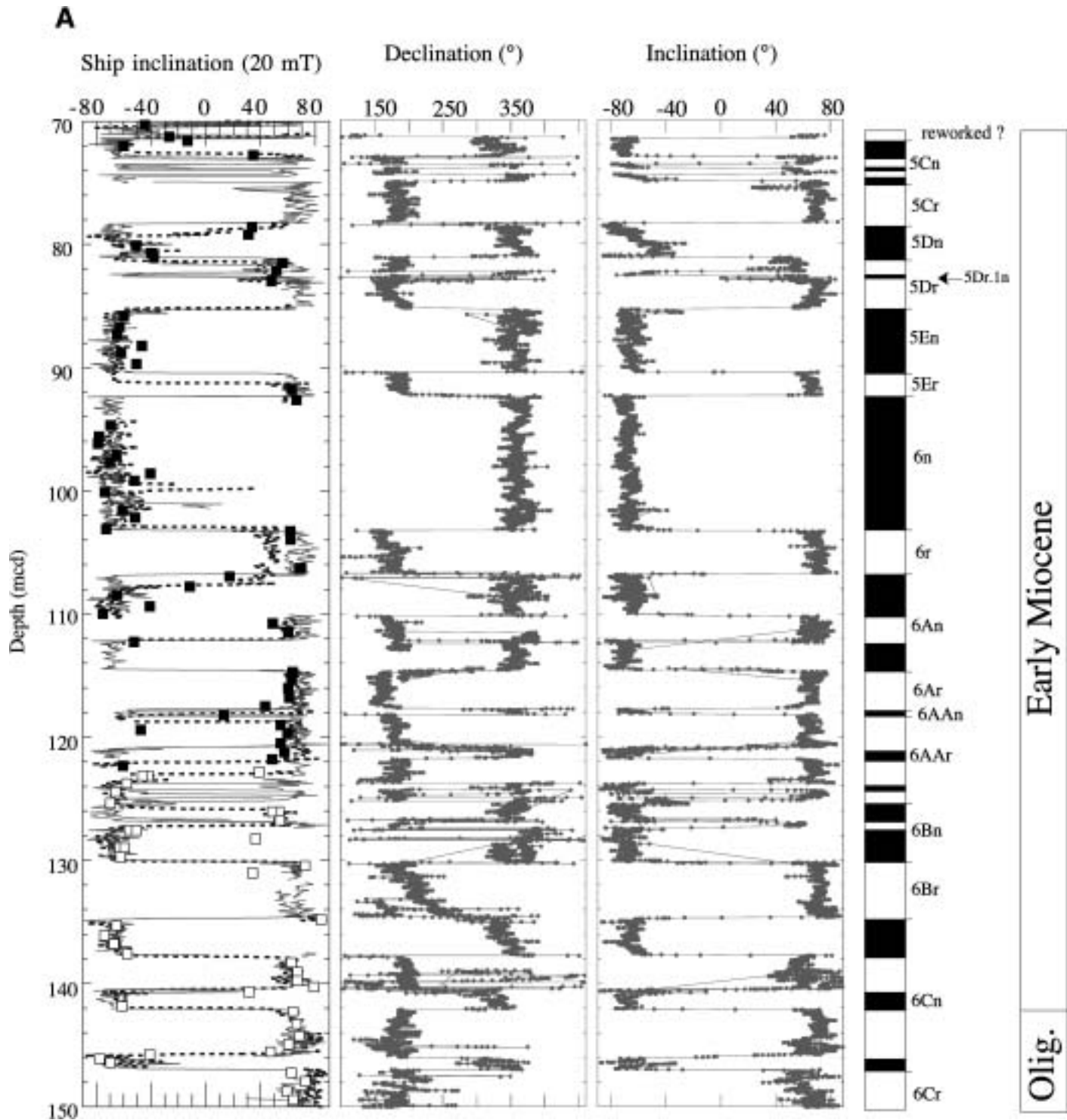


Figure 3. ODP Site 1090 u-channel, shipboard pass-through magnetometer, and discrete sample data for (A) the 70–150 mcd interval, and (B) the 150–230 mcd interval. Left column: Inclination data from shipboard pass-through measurements from Hole 1090B (dashed line) and Holes 1090D and 1090E (continuous lines) after demagnetization at peak fields of 20 mT. Squares are component inclinations determined from thermal (open squares) and alternating field (closed squares) demagnetization of discrete samples collected from Hole 1090B. Note that the Hole 1090B data are offset in the 115–127 mcd interval relative to the pass-through data from Holes 1090D and 1090E (continuous lines). This offset is attributed to imprecise hole-to-hole correlation by the Shipboard Scientific Party (1999). Center and right columns: Component declinations and inclinations from u-channel data calculated for the 20–80 mT demagnetization interval by using the standard least-squares method. All maximum angular deviation (MAD) values for these component directions are $<20^\circ$. Also shown is the correlation of polarity zones to polarity chrons for option 1 and for option 2 (labels in parentheses in Fig. 3B, right column) where this option differs from option 1.

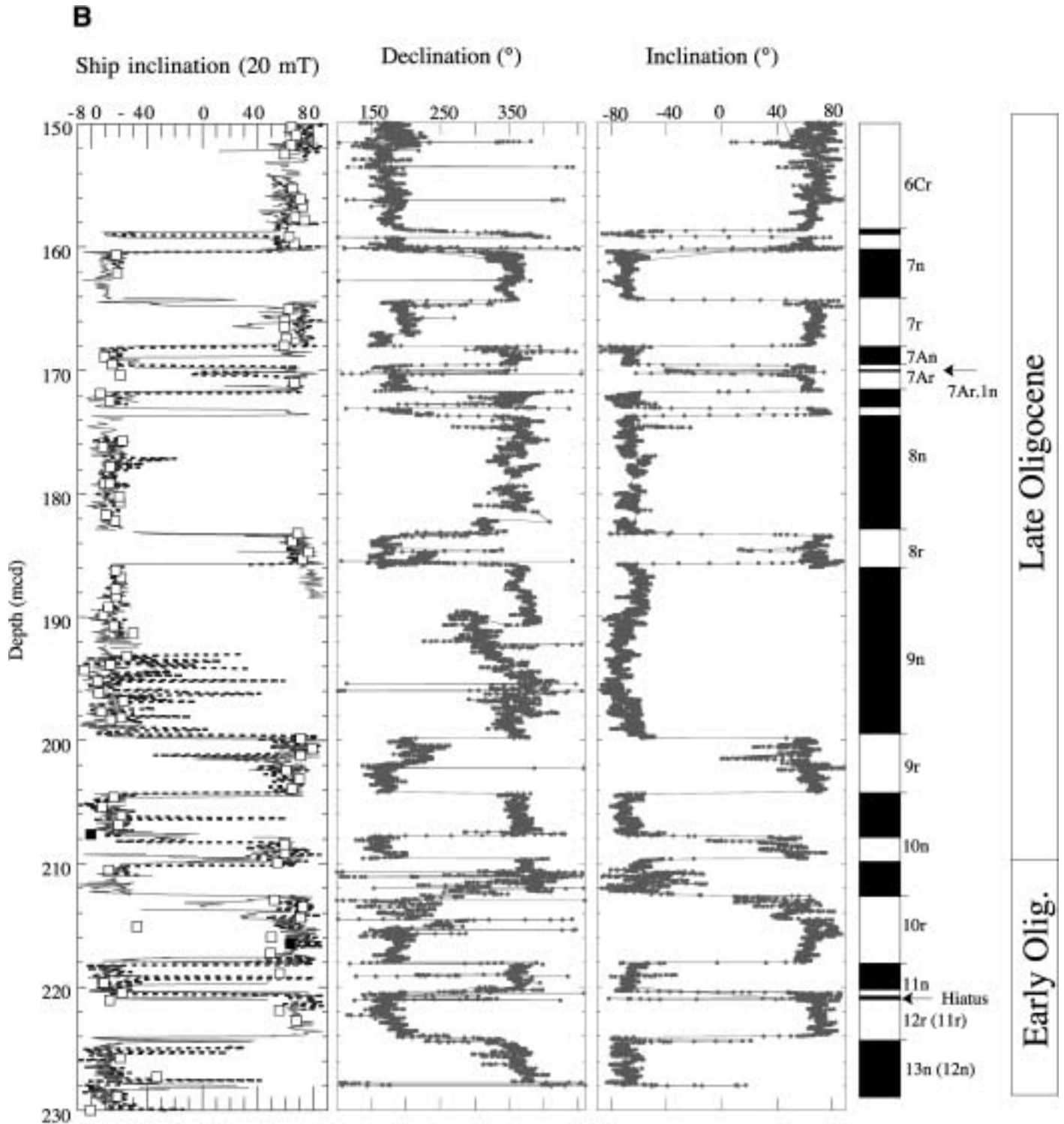


Figure 3. (Continued).

5, Table 1). The polarity-zone pattern fit is unambiguous above a hiatus at 221 mcd, marked by the coincidence of nanofossil events at this level (Marino and Flores, 2002a). Below the hiatus, in the C11n–C15n interval, there are two options for correlation to the GPTS.

The option 1 pattern fit (continuous tie lines in Fig. 5) is more compatible with the nanofossil biostratigraphy (Marino and Flores, 2002a, 2002b), whereas option 2 (dashed lines in Fig. 5) is more compatible with the foraminiferal biostratigraphy (Galeotti et al.,

2002). Preservation of nanofossils and foraminifera is discontinuous, and therefore the biostratigraphic arguments are not definitive. Although the polarity-zone pattern fit to polarity chrons of Cande and Kent is more obvious for option 2 (Fig. 5), we utilize $^{87}\text{Sr}/^{86}\text{Sr}$,

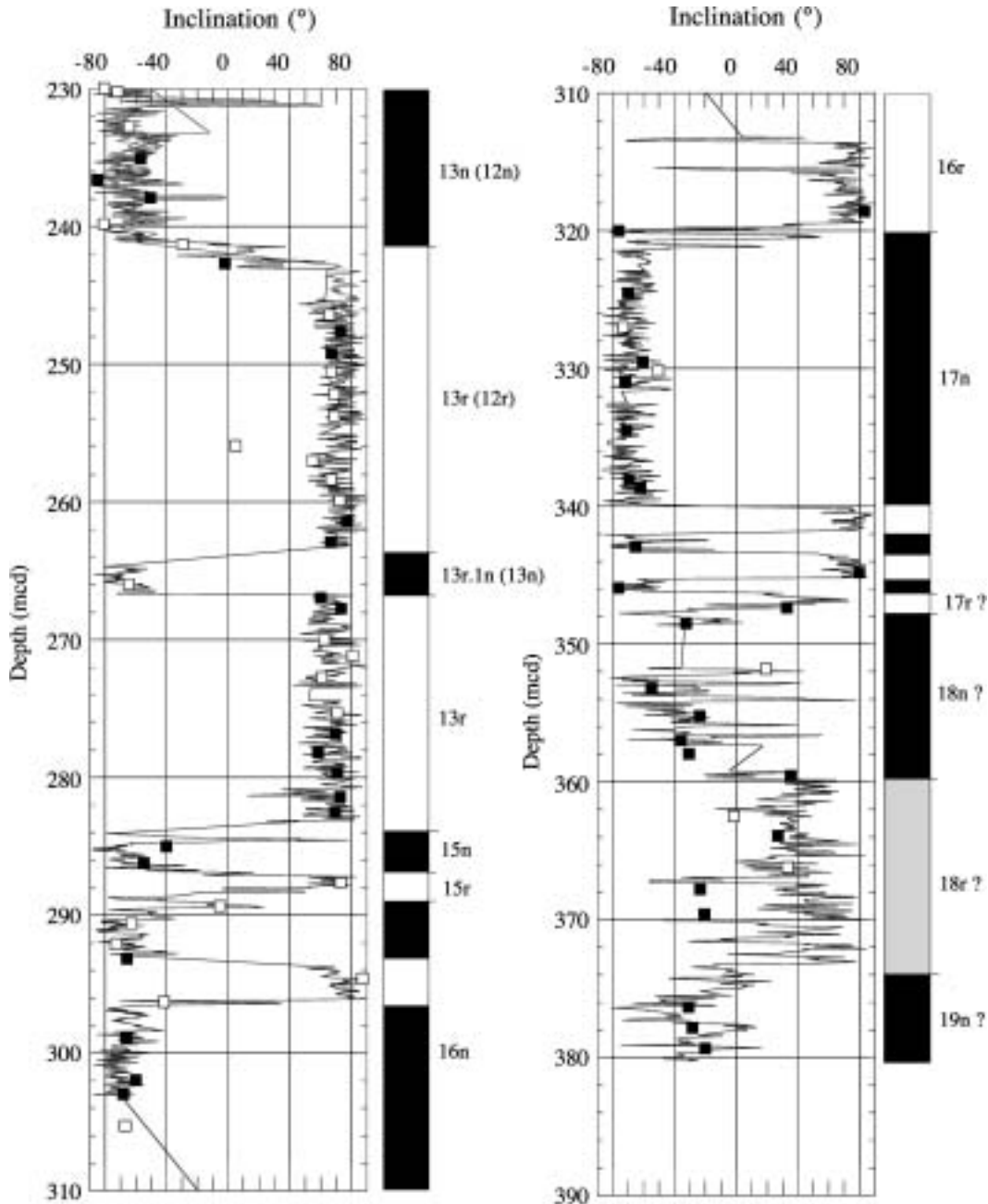


Figure 4. For the 230–380 mcd interval, below the level of u-channel sampling, the magnetostratigraphy is based on inclination data from shipboard pass-through measurements from Hole 1090B (dashed line) and Holes 1090D and 1090E (continuous lines) after demagnetization at peak fields of 20 mT. Component inclinations were determined from discrete samples from Hole 1090B after thermal (open squares) and alternating field (closed squares) demagnetization. Correlation of polarity zones to polarity chrons for option 1 and for option 2 (labels in parentheses) where this option differs from option 1.

$\delta^{13}\text{C}$, and $\delta^{18}\text{O}$ values, determined from planktic and benthic foraminifera, to show that option 1 is the correct choice.

Isotope Stratigraphy

Strontium isotope ratios were measured on foraminifera (calcite) from the 71.59 to 361.49

mcd interval at Site 1090. Strontium was separated from foraminifera by using Sr Spec resin and a technique modified from Pin and Bassin (1992). Blanks for this procedure are ~ 100 pg Sr. $^{87}\text{Sr}/^{86}\text{Sr}$ ratios were analyzed on a Micromass Sector 54 mass spectrometer. For each sample, 200 ratios were obtained at 1.5 V, and the isotope ratios were normalized to

$^{86}\text{Sr}/^{88}\text{Sr} = 0.1194$. Repeat analyses of the NBS987 standard yielded an $^{87}\text{Sr}/^{86}\text{Sr}$ ratio of 0.710240 with a 2σ uncertainty of ± 0.000023 .

Ages for $^{87}\text{Sr}/^{86}\text{Sr}$ data were determined from the magnetostratigraphic correlation to the GPTS of Cande and Kent (Table 2). Data are shown for interpretation option 1 (Table 2, Fig.

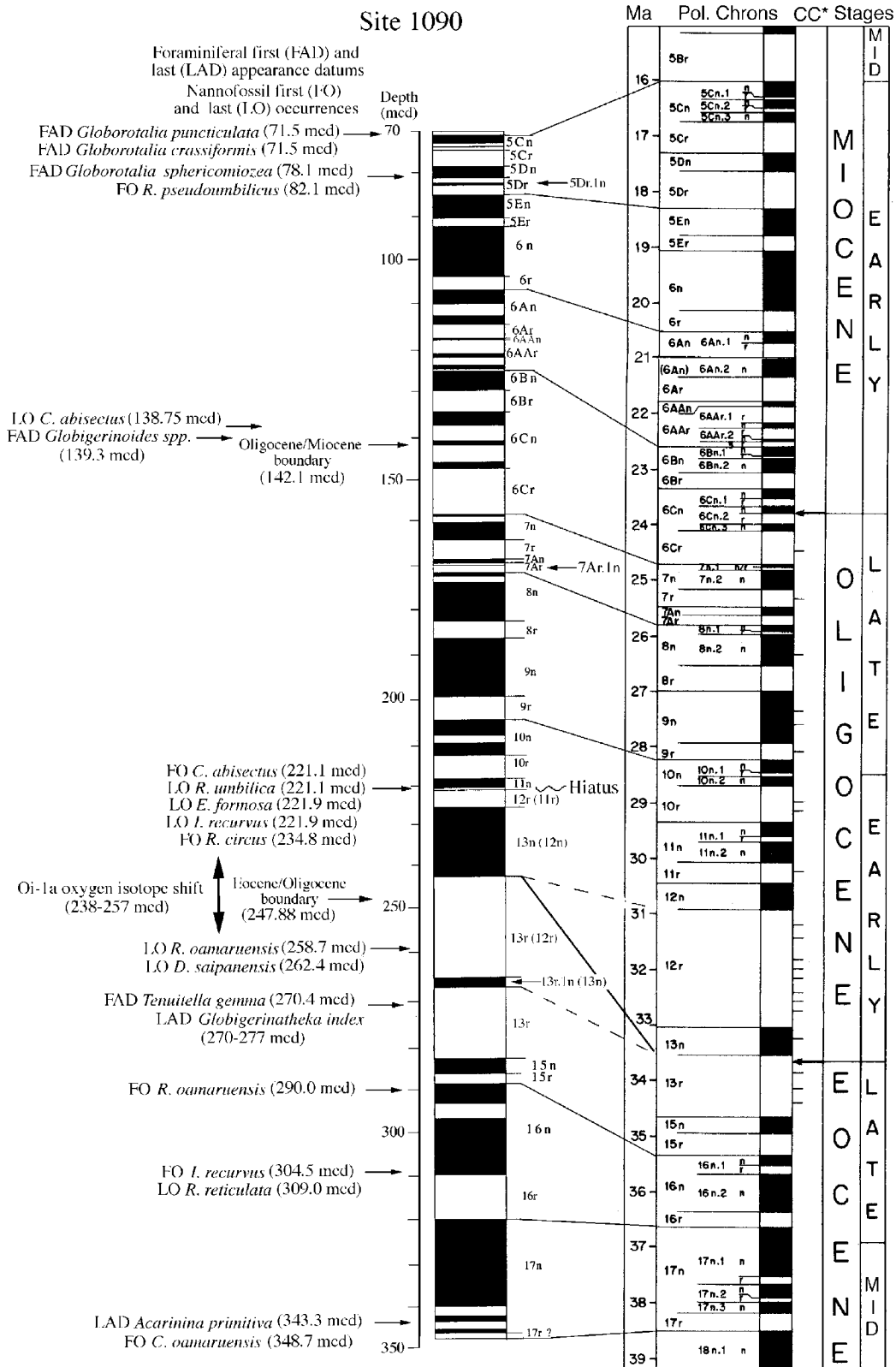


Figure 5. Correlation of the Site 1090 polarity stratigraphy to the Cande and Kent geomagnetic polarity time scale GPTS (Cande and Kent, 1992, 1995). CC* indicates “cryptochrons” in Cande and Kent time scale. Polarity zones at Site 1090 not correlative to polarity chrons in Cande and Kent (C5Dr.1n, C7Ar.1n, C13r.1n) are indicated. Correlation option 1 is shown as continuous tie lines, and the variant option 2 is shown as dashed tie lines. Option 2 polarity chron labels are in parentheses where they differ from option 1 labels. Foraminiferal and nannofossil events after Galeotti et al. (2002) and Marino and Flores (2002a, 2002b, 2002c). Oi-1a isotopic shift occurs in the 238–257 mcd interval.

TABLE 1. DEPTHS OF POLARITY ZONES IN METERS COMPOSITE DEPTH (MCD) AT SITE 1090 AND CORRELATIVE POLARITY-CHRON LABELS

Normal polarity chron boundaries	Age (Ma)*	Age (Ma)**	Age offset (m.y.)	Depth at Site 1090 (mcd)
C5Cn.1n	16.014	15.895	0.12	71.40
C5Cn.1n	16.293	16.147	0.15	72.90
C5Cn.2n	16.327	16.178	0.15	73.50
C5Cn.2n	16.488	16.323	0.17	73.88
C5Cn.3n	16.556	16.384	0.17	74.40
C5Cn.3n	16.726	16.538	0.19	74.95
C5Dn	17.277	17.035	0.24	78.30
C5Dn	17.615	17.340	0.28	81.10
C5Dr.1n		17.501		82.28
C5Dr.1n		17.556		82.60
C5En	18.281	17.941	0.34	85.28
C5En	18.781	18.392	0.39	90.42
C6n	19.048	18.633	0.42	92.30
C6n	20.131	19.610	0.52	103.30
C6An.1n	20.518	19.959	0.56	106.77
C6An.1n	20.725	20.146	0.58	110.20
C6An.2n	20.996	20.390	0.61	112.30
C6An.2n	21.320	20.682	0.64	114.60
C6AAn	21.768	21.087	0.68	117.70
C6AAn	21.859	21.169	0.69	118.15
C6AAr.1n	22.151	21.432	0.72	120.80
C6AAr.1n	22.248	21.520	0.73	121.76
C6AAr.2n	22.459	21.710	0.75	123.80
C6AAr.2n	22.493	21.741	0.75	124.30
C6Bn.1n	22.588	21.827	0.76	125.10
C6Bn.1n	22.750	21.973	0.78	126.90
C6Bn.2n	22.804	22.021	0.78	127.35
C6Bn.2n	23.069	22.260	0.81	130.25
C6Cn.1n	23.353	22.517	0.84	134.65
C6Cn.1n	23.535	22.681	0.85	137.72
C6Cn.2n	23.677	22.809	0.87	140.50
C6Cn.2n	23.800	22.920	0.88	142.10 [§]
C6Cn.3n	23.999	23.137	0.86	145.90
C6Cn.3n	24.118	23.266	0.85	147.00
C7n.1n	24.730	23.933	0.80	158.75
C7n.1n	24.781	23.988	0.79	159.25
C7n.2n	24.835	24.047	0.79	160.35
C7n.2n	25.183	24.426	0.76	164.35
C7An	25.496	24.767	0.73	168.10
C7An	25.648	24.932	0.72	169.62
C7Ar.1n		24.965		170.00
C7Ar.1n		24.994		170.33
C8n.1n	25.823	25.123	0.70	171.80
C8n.1n	25.951	25.262	0.69	173.12
C8n.2n	25.992	25.307	0.69	173.70
C8n.2n	26.554	25.919	0.64	183.35
C9n	27.027	26.434	0.59	185.70
C9n	27.972	27.463	0.51	199.85
C10n.1n	28.283	27.801	0.48	204.30
C10n.1n	28.512	28.051	0.46	207.80
C10n.2n	28.578	28.123	0.46	209.60
C10n.2n	28.745	28.305	0.44	212.60
C11n.1n	29.401	29.019	0.38	218.05
Hiatus				
C13n	33.058	33.001	0.06	224.00
C13n	33.545	33.531	0.01	242.00 [†]
C13r (.14)				247.88 [†]
C15n	34.655			284.00 [†]
C15n	34.940			287.00 [†]
C16.1n	35.343			289.00 [†]
C16.1n	35.526			293.50 [†]
C16n.2n	35.685			296.00 [†]
C16n.2n	36.341			309.00 [†]
C17n.1n	36.618			319.80 [†]
C17n.1n	37.473			340.00 [†]
C17n.2n	37.604			342.00 [†]
C17n.2n	37.848			343.50 [†]
C17n.3n	37.920			345.00 [†]

*Age of polarity chrons is from Cande and Kent (1992, 1995).

**Ages rescaled to the Shackleton et al. (2000) age (22.92 Ma) for the Oligocene/Miocene (O/M) boundary.

†Shipboard and discrete sample data only (no u-channel data in this interval).

‡Estimated depth of Eocene/Oligocene boundary.

§Estimated depth of Oligocene/Miocene boundary.

TABLE 2. CORRELATION OF SITE 1090 Sr ISOTOPE DATA TO AGE USING CANDE AND KENT (1992, 1995) TIME SCALE

Age (Ma)	⁸⁷ Sr/ ⁸⁶ Sr	Age (Ma)	⁸⁷ Sr/ ⁸⁶ Sr
16.087	0.708727	27.303	0.708046
16.180	0.708714	27.377	0.708041
16.502	0.708688	27.430	0.708026
16.733	0.708671	27.463	0.708059
16.744	0.708671	27.528	0.708034
16.744	0.708644	27.530	0.708046
16.782	0.708666	27.577	0.708046
16.963	0.708639	27.654	0.708048
17.094	0.708634	27.660	0.708042
17.111	0.708648	27.661	0.708040
17.242	0.708642	27.663	0.708040
17.259	0.708635	27.677	0.708046
17.492	0.708632	27.692	0.708044
17.628	0.708604	27.728	0.708048
17.771	0.708596	27.778	0.708058
17.242	0.708733	27.784	0.708031
17.962	0.708617	28.072	0.708012
18.026	0.708598	29.534	0.707965
18.042	0.708581	29.534	0.707939
18.249	0.708594	33.066	0.707840
18.544	0.708562	33.092	0.707817
18.681	0.708521	33.310	0.707812
18.749	0.708536	33.449	0.707812
20.124	0.708474	33.457	0.707792
22.485	0.708284	33.576	0.707802
22.487	0.708302	33.968	0.707793
22.740	0.708303	33.968	0.707805
22.740	0.708272	34.633	0.707775
23.248	0.708260	35.539	0.707754
23.345	0.708264	36.087	0.707764
23.489	0.708236	36.648	0.707732
23.839	0.708237	37.013	0.707721
24.045	0.708178	37.235	0.707727
25.986	0.708127	37.703	0.707726
26.074	0.708107	37.800	0.707747
26.277	0.708089	37.907	0.707704
26.508	0.708079	38.268	0.707712
26.665	0.708080	39.222	0.707730
26.697	0.708058	39.222	0.707744
26.902	0.708049	39.573	0.707735
26.902	0.708077	40.085	0.707728
27.231	0.708057	40.619	0.707758
27.277	0.708069		

6) and for option 2 where the ages differ (open circles in Fig. 6). Continuous lines in Figure 6 represent the ± 0.000023 uncertainty bands surrounding a ninth-order polynomial applied to the seawater data from Hodell and Woodruff (1994), Mead and Hodell (1995), and Martin et al. (1999). ⁸⁷Sr/⁸⁶Sr data from Site 1090 fall within the uncertainty of the seawater curve for option 1, thereby supporting this option.

The Miocene-late Oligocene (15–27 Ma) benthic carbon and oxygen isotope data at Site 1090 were generated from *Cibicidoides* spp. and *Oridorsalis* spp. (Billups et al., 2002). Foraminifera are rare, and large (40 cm³) samples were necessary to obtain sufficient specimens. The *Oridorsalis* $\delta^{13}\text{C}$ and $\delta^{18}\text{O}$ data were corrected to *Cibicidoides* values on the basis of 79 measurements of both species from the same levels ($\delta^{18}\text{O}$ correction: -0.4‰ , $\delta^{13}\text{C}$ correction: $+1.3\text{‰}$). These Miocene-late Oligocene data of Billups et al. (2002) were supplemented by samples collected from close

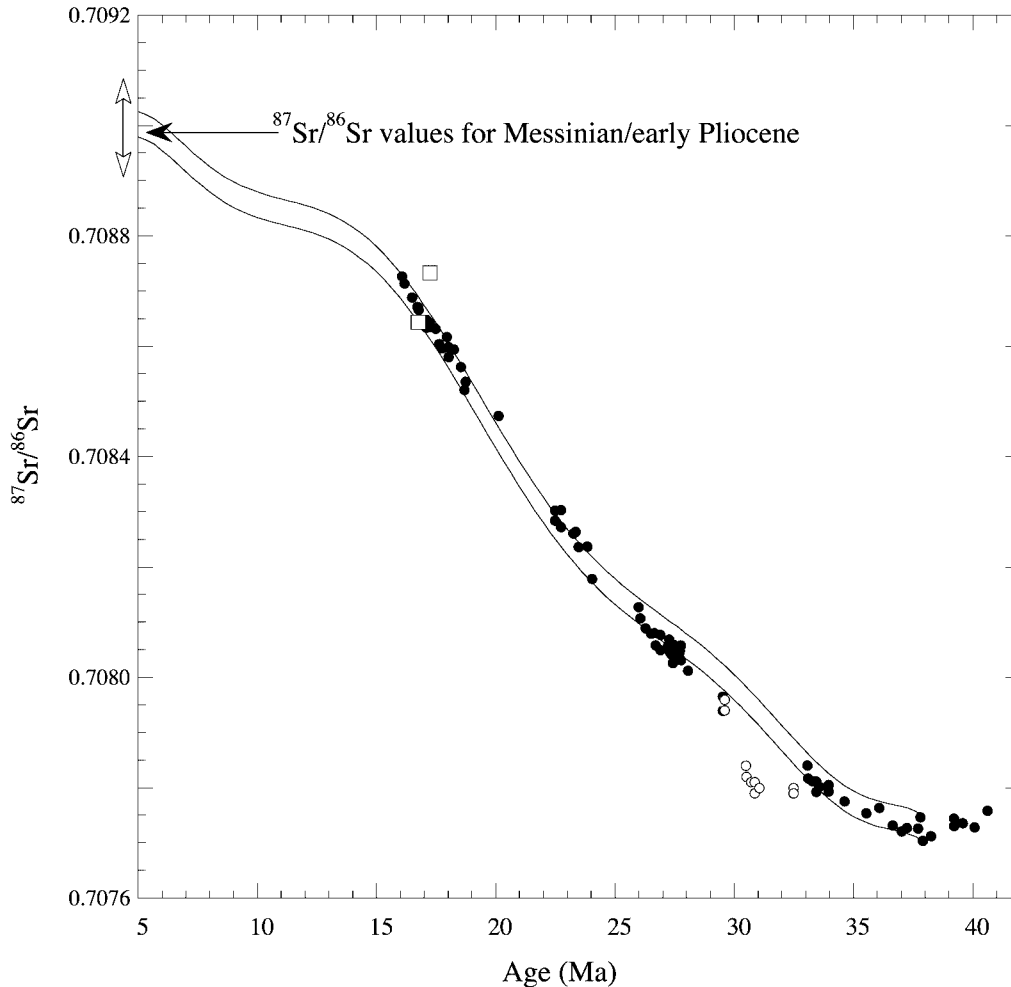


Figure 6. Strontium isotope data from ODP Site 1090 for bulk foraminifera (open and closed circles) and for foraminifera identified as *Globorotalia sphericomiozea* (open squares). Age model for Site 1090 based on correlation of polarity zones to the Cande and Kent (1992, 1995) geomagnetic polarity time scale. Closed circles and open squares indicate data placed on an age model consistent with polarity interpretation option 1. Open circles indicate the same data placed on an age model consistent with polarity interpretation option 2, where the two options differ. Continuous lines represent the ± 0.00023 uncertainty window for a ninth-order polynomial applied to the seawater data from Hodell and Woodruff (1994), Mead and Hodell (1995), and Martin et al. (1999). Analytical error is equal to the size of the circular symbols.

to the Eocene/Oligocene boundary. For this interval, specimens of *Cibicidoides* spp. were picked from 30 cm³ samples. Bulk sediment was washed through a 63 μ m sieve, and specimens were soaked in 15% hydrogen peroxide for 20 min, then sonicated for 5 min with methanol. Specimens were oven dried, and then reacted in orthophosphoric acid at 70 °C in a Finnigan-MAT Kiel III carbonate preparation device. Isotopic ratios of purified CO₂ gas were measured on-line with a Finnigan-MAT at the University of Florida. Analytical precision is better than $\pm 0.1\%$ for $\delta^{18}\text{O}$. Isotope data were calibrated by using the NIST/NBS (U.S. National Institute of Standards and Technology/National Bureau of Standards) 19

standard, and values are reported relative to PDB (Peedee belemnite).

Comparison of the $\delta^{13}\text{C}$ and $\delta^{18}\text{O}$ data from Site 1090 with the compilation of Zachos et al. (2001a), derived from 40 DSDP and ODP sites calibrated in accordance with the Cande and Kent time scale (Fig. 7), indicates that the Site 1090 isotopic data are consistent with the magnetostratigraphically derived age model. The two interpretations (option 1 and option 2) differ only in the vicinity of the Eocene/Oligocene boundary (Figs. 5 and 8). The stable isotope shift close to the Eocene/Oligocene boundary, termed Oi-1 by Miller et al. (1991), is detected in the 238–257 mcd interval (Fig. 5), corresponding to 33–34 Ma on

the Cande and Kent time scale (Fig. 7). As we expect this isotopic shift to lie close to the C13r/C13n boundary (see Salamy and Zachos, 1999), its position favors interpretation option 1 (Fig. 5). The $\delta^{13}\text{C}$ and $\delta^{18}\text{O}$ (Oi-1a) shifts at Site 1090, when placed on the Cande and Kent time scale by using option 1 (closed symbols in Fig. 7), are consistent with the Zachos et al. (2001a) compilation for seawater $\delta^{13}\text{C}$ and $\delta^{18}\text{O}$. On the other hand, the shift is too young when using option 2 (open symbols in Fig. 7). Note that Site 1090 $\delta^{18}\text{O}$ values in Figure 7 have been adjusted by +0.64 to bring foraminiferal data to seawater values and account for disequilibrium vital effects (Shackleton, 1974).

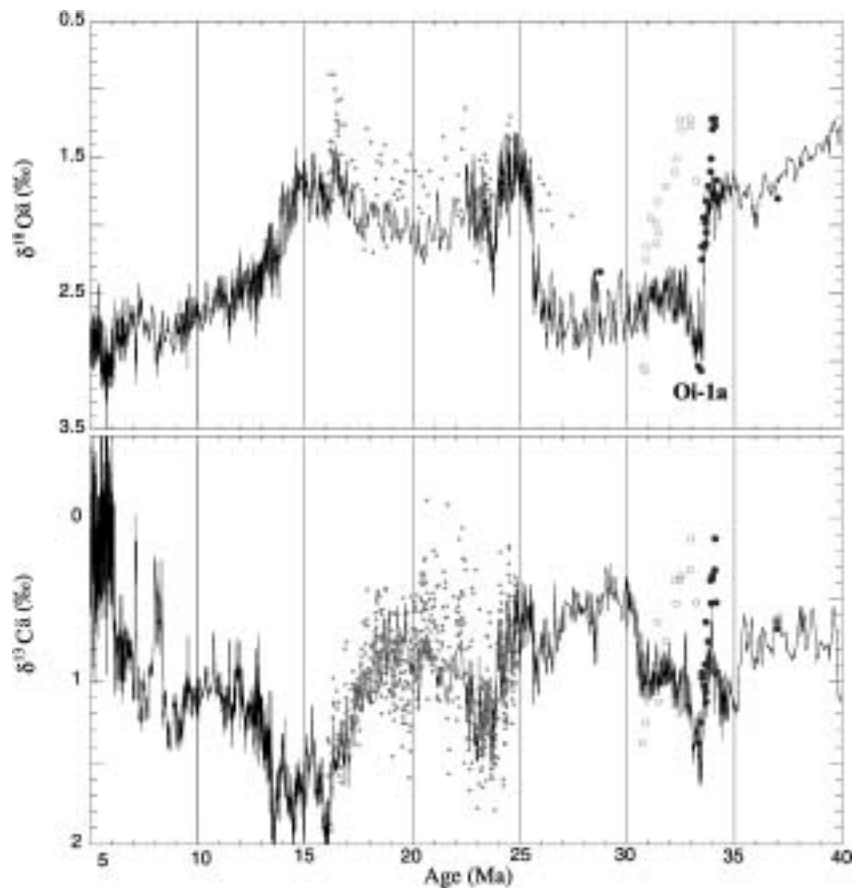


Figure 7. Oxygen and carbon isotope data from ODP Site 1090 (Billups et al., 2002) (small closed points) superimposed on the composite curves of Zachos et al. (2001a) derived from 40 DSDP and ODP sites (continuous line). All data placed on age model by using the Cande and Kent (1992, 1995) geomagnetic polarity time scale. The isotopic shifts at the Eocene/Oligocene boundary (33.7 Ma per Cande and Kent) are consistent with polarity-zone-correlation option 1 (closed symbols) rather than option 2 (open symbols).

Biostratigraphy

Established correlation of calcareous bioevents to the GPTS at Southern Ocean sites can be used to test the interpretation of the magnetostratigraphy at Site 1090 (Fig. 5, Table 3). Outstanding among the Southern Ocean magnetostratigraphic studies are those from north of the Walvis Ridge drilled during DSDP Leg 73 (Tauxe et al., 1983, 1984) and ODP Site 689 from the Maud Rise (Speiß, 1990). Owing to the relative clarity of these magnetostratigraphic results, both the biostratigraphic studies of DSDP Leg 73 strata (Poore et al., 1984) and at ODP Site 689 (Wei and Wise, 1990; Stott and Kennett, 1990) take on special significance. In contrast, the detailed nannofossil studies at Holes 744A and 748B (ODP Leg 119/120, Kerguelen Plateau) (Wei and Thierstein, 1991; Wei et al., 1992) are hampered by poorly defined magnetostratigraphic

intervals (Keating and Sakai, 1991; Inokuchi and Heider, 1992). Similarly, the nannofossil biostratigraphic results of Wei (1991) from ODP Leg 114 (Sites 699 and 703) are not easily correlated to the GPTS because of poorly defined magnetostratigraphic intervals (Hailwood and Clement, 1991a, 1991b). DSDP Site 516 and other DSDP Leg 72 sites have Cenozoic magnetostratigraphic intervals that are very difficult to interpret, leading to equivocal biomagnetostratigraphic correlations (Berggren et al., 1983; Wei and Wise, 1989).

The first occurrence (FO) of *C. oamaruensis* lies at 348.7 mcd near the base of the magnetostratigraphic section close to the onset of C17r (Fig. 5). The event occurs in C17n.1n at DSDP Site 523 (Poore et al., 1984). The datum probably correlates to C17n at ODP Site 689 (Wei and Wise, 1990), although the interpretation of the magnetostratigraphy at this level at Site 689 is equivocal (Speiß, 1990).

The last occurrence (LO) of the foraminifer *A. primitiva* lies below the FO of *C. oamaruensis* at Site 689, in a polarity chron interpreted as C18 (Stott and Kennett, 1990). At Site 1090, the LO of *A. primitiva* is recorded at 343.26 mcd in an interval correlative to C17n.2n.

The LO of *R. reticulata* lies in C16n.2n at Site 1090, consistent with its occurrence at ODP Site 689 (Wei and Wise, 1990). The FO of *I. recurvus* at 304.5 mcd (Fig. 5) confirms the magnetostratigraphic interpretation at Site 1090 in this interval. This datum occurs consistently in C16n at DSDP Site 522 (Poore et al., 1984), at ODP Site 689 (Wei and Wise, 1990), in the Contessa section (Lowrie et al., 1982), and in the Bottaccione Gorge at Gubbio (Monechi and Thierstein, 1985).

The FO of *R. oamaruensis* occurs in C16n.1n at Site 1090, which is consistent with the result from Sites 689 and 744 (Wei and Wise, 1990; Wei et al., 1992; Speiß, 1990). The LO of *R. reticulata* is also correlated to C16n at these sites, as well as at Site 703 (Wei, 1991), and to C16n.2n at Site 1090.

The LO of *R. oamaruensis* is thought to be a useful marker for the Eocene/Oligocene boundary, particularly at high southerly latitudes where sphenoliths are absent. At Site 689 (ODP Leg 113), the event is correlated to C13r (Wei and Wise, 1990; Speiß, 1990) and is reported to occur at the C13r/C13n boundary at Site 699 (Wei, 1991). This marker occurs at 259 mcd, within C13r, at Site 1090 (Fig. 5).

The LO of *D. saipanensis* is thought to be diachronous between low-mid and high southerly latitudes (Berggren et al., 1995). The occurrence at Site 1090 within C13r is consistent with Italian land sections (Nocchi et al., 1986; Premoli Silva et al., 1988; Coccioni et al., 1988).

The LO of *G. index* is reported to occur within the uppermost part of C16n at Site 689 (Stott and Kennett, 1990). However, a reinterpretation of the magnetostratigraphy at Sites 689 and 690 (Berggren et al., 1992) led to the conclusion that the LO of this taxon falls in C15n at these sites. In the Contessa section this event is recorded in C13r (Nocchi et al., 1986; Premoli Silva et al., 1988). According to Berggren et al. (1995), the LAD of *G. index* is recorded in the older half of C13r at an absolute age of ca. 34.3 Ma, slightly predating the Eocene/Oligocene boundary. At Site 1090, the LAD of *G. index* occurs in the older half of C13r.

The FAD of *Tenuitella gemma* is recorded at Site 1090 just above, or in coincidence with, the exit of *G. index*. According to Radford and Li (1993), *Tenuitella* evolved from

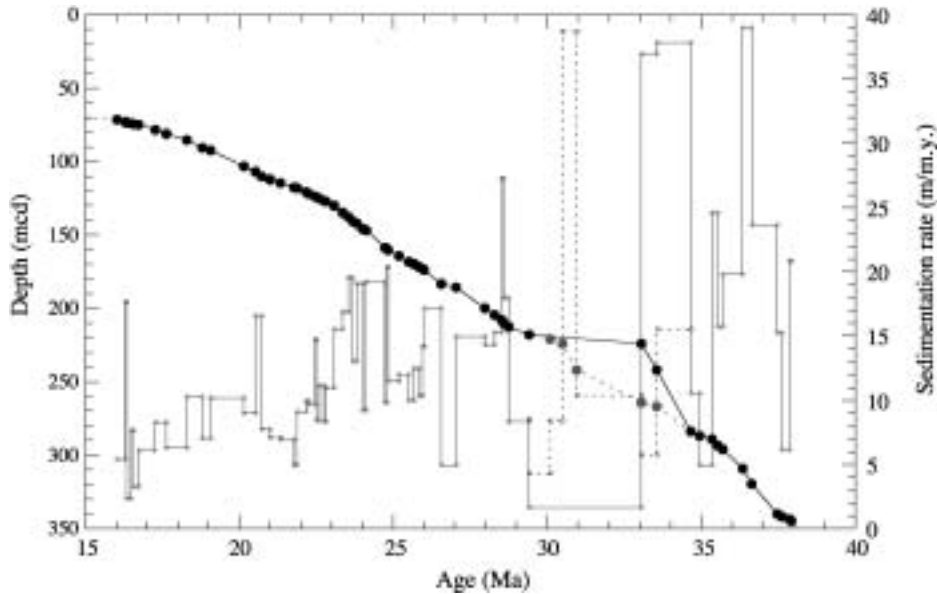


Figure 8. Age vs. depth relationship and sedimentation rates for the 70–350 mcd (16–38 Ma) interval at Site 1090 based on correlation of the polarity record to the Cande and Kent (1992, 1995) time scale. Option 1 (preferred) is shown as continuous lines; option 2 is shown as dashed lines (see text for explanation).

TABLE 3. DEPTHS AND AGES OF BIOSTRATIGRAPHIC EVENTS AND THE OI-1A ISOTOPE EVENT

Event	Depth at Site 1090 (mcd)	Polarity chron	Age at Site 1090 (Ma)	Age from Berggren et al. (1995) (Ma)
Foraminifera (Galeotti et al., 2002)				
FO <i>Globorotalia sphericomiozea</i>	78.05	5Cr	17.24	5.6
FO <i>Globigerinoides</i> spp.	139.26	6Cn.1r	23.61	
FO <i>Catapsydrax dissimilis</i> s.s.	243.09	13r	33.57	
FO <i>Tenuitella gemma</i>	270.36	13r	34.30	
LO <i>Globigerinatheka index</i>	270–277	13r	34.3–34.5	34.3
LCO <i>Nuttallides truempyi</i>	320.00	17n/16r	36.63	
LO <i>Acarinina primitiva</i>	343.26	17n.2n	37.81	39.0
Nannofossils (Marino and Flores, 2002a, 2002b, 2002c)				
LO <i>Cyclicargolithus abisectus</i>	138.75	6Cn.1r	23.59	
LO <i>Reticulofenestra umbilica</i>	221.14	12r-11n	Hiatus (29.4–33.1)	31.3
FO <i>Cyclicargolithus abisectus</i>	221.14	12r-11n	Hiatus (29.4–33.1)	
LO <i>Isthmolithus recurvus</i>	221.89	12r-11n	Hiatus (29.4–33.1)	31.8–33.1
LO <i>Ericsonia formosa</i>	221.89	12r-11n	Hiatus (29.4–33.1)	32.8
FO <i>Reticulofenestra circus</i>	234.81	13n	33.35	
LO <i>Reticulofenestra oamaruensis</i>	258.69	13r	33.99	33.7
LO <i>Discoaster saipanensis</i>	262.39	13r	34.08	34.2
FO <i>Reticulofenestra oamaruensis</i>	289.96	16n.1n	35.38	35.4
FO <i>Isthmolithus recurvus</i>	304.51	16n.2n	36.11	36.0
LO <i>Reticulofenestra reticulata</i>	308.97	16n.2n	36.34	36.1
FO <i>Chiasmolithus oamaruensis</i>	348.73	18n/17r	38.4	37.0
Oi-1a [†]	238–257	13r-13n	33.44–33.94	

[†]For other oxygen and carbon isotope events at Site 1090, see Billups et al. (2002).

Praetenuitella in the earliest Oligocene. The plexus originates with *T. gemma* after the global extinction of *G. index*. In a short interval of relatively clear magnetostratigraphy across the Eocene/Oligocene boundary at ODP Site 748, the FO of *T. gemma* is recorded in what is interpreted as C13n (Berggren, 1992). This bioevent occurs in the older half of C13r at Site 1090.

The last appearances of four nannofossil

species (*C. abisectus*, *R. umbilica*, *E. formosa*, and *I. recurvus*) occur at ~221 mcd at Site 1090, at a postulated hiatus incorporating the interval between C12r and C11n, including parts of these two polarity chrons (Fig. 5). The LO of *I. recurvus* is found in the upper part of C13n at Hole 522, in C12r at Hole 523, and in C12r in the Contessa section (Poore et al., 1984; Lowrie et al., 1982). It appears that the LO of *E. formosa* can be as old as C18 on

the Kerguelen Plateau, although its mid- to low-latitude correlation is to C12r (Berggren et al., 1995). The LO of *R. umbilica* is also correlated to C12r at DSDP Sites 522 and 523 (Poore et al., 1984) and in the Contessa section (Lowrie et al., 1982).

The LO of *Cyclicargolithus abisectus* lies close to the Oligocene/Miocene boundary in the South Atlantic and Indian Oceans (Fornaciari et al., 1990; Wei, 1991; Poore et al., 1984), and in the Contessa land section (Lowrie et al., 1982). The nannofossil subzone of the same name is the uppermost subzone of the Oligocene in the zonation of Bukry (1973), who placed the Oligocene/Miocene boundary at the termination of the acme of this species. At Site 1090, the LO of *C. abisectus* at 138.75 mcd in C6Cn.1r places it in the earliest Miocene, 3.4 m above the Oligocene/Miocene boundary (Fig. 5). Close to the LO of *C. abisectus*, the first common occurrence of *Globigerinoides* characterizes the planktic foraminiferal assemblage. The development of *Globigerinoides* spp. is a characteristic element of lowermost Miocene faunas, used by Blow (1969) to define the P22/N4 zonal boundary. At Site 1090, this bioevent occurs in C6Cn.1r in an interval characterized by poor preservation of planktic foraminifera.

High-resolution sampling at ~10 cm intervals from 71 to 89 mcd spans the section containing specimens of foraminifera identified as *Globorotalia sphericomiozea*. The FO of this species is at 78.05 mcd (Fig. 5). According to Hornibrook et al. (1989), *G. sphericomiozea* is an intermediate form in the evolution of *Globorotalia conoidea* and *Globorotalia puncticulata*. The New Zealand range of this species is reported by the same authors to span the upper part of the Kapitean (latest Messinian to the lower part of the Zanclean). As summarized in Jenkins (1993), *G. sphericomiozea* first appears at the base of the *G. conomiozea* Zone in the southern mid-latitude biozonation of Jenkins (1971, 1975, 1978). Scott et al. (1990) reported that *G. sphericomiozea* has a short stratigraphic range spanning the upper part of the Kapitean and the Miocene/Pliocene boundary in New Zealand. According to Berggren et al. (1995), the FAD of *G. sphericomiozea* falls in C3r at ca. 5.6 Ma. The first appearance of *G. sphericomiozea* at 78.05 mcd at Site 1090 should therefore be indicative of a latest Miocene–early Pliocene age.

Figure 6 indicates the range of ⁸⁷Sr/⁸⁶Sr values associated with the conventional Messinian–early Pliocene age range of *G. sphericomiozea*. Two samples of specimens identified as *G. sphericomiozea* from 75.06 and 78.06 mcd were an-

alyzed for Sr isotopes. These samples yielded $^{87}\text{Sr}/^{86}\text{Sr}$ values of 0.708644 and 0.708733 and are plotted as open squares in Figure 6. These values are consistent with an early Miocene age. Strontium isotope values for other foraminifera from this depth range also indicate an early Miocene age. The *G. sphericomiozea* specimens were not, therefore, mixed down-section (Fig. 6).

The $\delta^{13}\text{C}$ and $\delta^{18}\text{O}$ data from Site 1090 (Billups et al., 2002), when placed on the magnetostratigraphic age model, are consistent with the global composite of Zachos et al. (2001a) (Fig. 7). The $\delta^{13}\text{C}$ and $\delta^{18}\text{O}$ data younger than 17.5 Ma (<80 mcd) cannot be easily reconciled with the Messinian to Pliocene (~5 m.y.) part of the composite curve (Fig. 7). The Sr, $\delta^{13}\text{C}$, and $\delta^{18}\text{O}$ data are therefore inconsistent with the presence of a supposedly Messinian–Pliocene foraminifer (*G. sphericomiozea*) in the top 10 m of the sampled section at Site 1090.

As reported by Scott et al. (1990), *G. sphericomiozea* is characterized by a large intraspecific variability, including the presence/absence of keeled morphotypes. According to Kennett and Srinivasan (1983), *G. sphericomiozea* forms part of the *Globoconella* lineage that originated from *Paragloboconella nana* in the early Miocene. The *Globoconella* series is a major lineage in temperate areas and very useful for biostratigraphic subdivision. Of the *Globoconella* lineage sensu Kennett and Srinivasan (1983), early Miocene–middle Miocene species showing a close similarity with *G. sphericomiozea* are *Globoconella miozea*, *Globoconella zealandica*, and *Globoconella amuria*. The last of these, in particular, closely resembles the unkeeled morphotype of *G. sphericomiozea*, although it has four and one-half to five chambers in the last whorl instead of four, and a less extended lower aperture. As the specimens identified at Site 1090 show four chambers in the last whorl and a relatively high-arched aperture (Fig. 9), they fall within the range of intraspecific variability of *G. sphericomiozea*. The ages implied by the $^{87}\text{Sr}/^{86}\text{Sr}$, $\delta^{13}\text{C}$, and $\delta^{18}\text{O}$ data, and the magnetostratigraphic interpretation, lead us to consider a continuum in morphological variation with the early Miocene–middle Miocene *G. amuria*. Alternatively, our specimens may fall into the intraspecific variability of *G. zealandica*, the LAD of which is reported to fall within chron C5Dn at 17.3 Ma by Berggren et al. (1995). The specimens occurring at Site 1090 show a somewhat less subquadrate profile and a slightly higher aperture than *G. zealandica*. Some specimens also show an inflated dorsal side with development of a small dome,

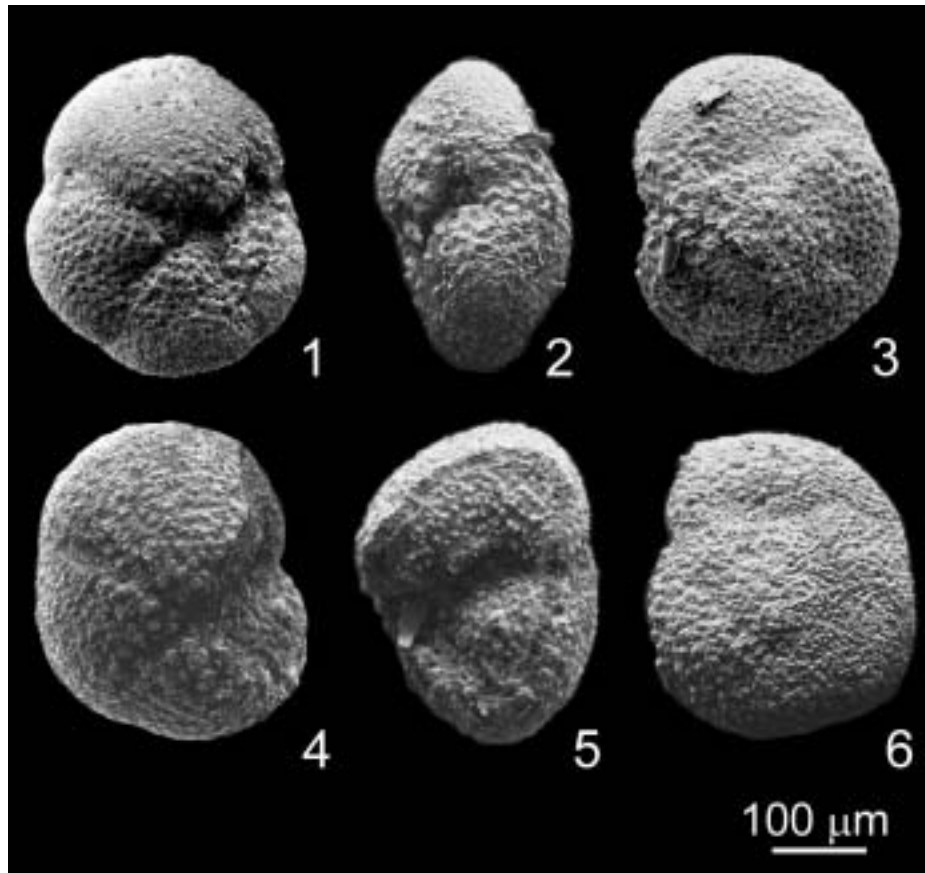


Figure 9. Scanning-electron microscope images of specimens, identified as *Globoconella sphericomiozea*, from the upper part of the studied interval at Site 1090. 1–3: *Globoconella sphericomiozea* Walters (biconvex morphotype), sample 1090D–8H–4, 24–26 cm (75.12 mcd). 4–6: *Globoconella sphericomiozea* Walters (planoconvex morphotype), sample 1090D–8H–4, 24–26 cm (75.12 mcd). The two specimens illustrated are representative of the intraspecific variability within the assemblage, which is typical for *G. sphericomiozea*. The occurrence of this taxon is indicative of a late Miocene–early Pliocene age, although the $^{87}\text{Sr}/^{86}\text{Sr}$ data (Fig. 6), $\delta^{13}\text{C}$ and $\delta^{18}\text{O}$ data (Fig. 7), and magnetostratigraphy (Fig. 5) indicate an early Miocene–middle Miocene age.

whereas *G. zealandica* generally shows a rather flattened dorsal side. Further studies and comparison with material from other localities is necessary to better understand the taxonomy and biostratigraphic significance of our Site 1090 specimens.

The unconformity at ~71 mcd separating the reddish nannofossil oozes of (mainly) early Miocene age from the white nannofossil oozes of Pliocene age is marked by a 45-cm-thick black/gray, partly laminated, tephra. The reddish-mottled white nannofossil ooze in the 50 cm immediately below the tephra contains abundant ash grains, as well as the Pliocene foraminifera *G. puncticulata* and *G. crassaformis* that are identified in a sample from 71.5 mcd (Galeotti et al., 2002). In this interval, only rare to scattered forms can be considered to be in situ; the rest of the assemblage

comprises reworked forms ranging in age from the Late Cretaceous (Campanian–Maastrichtian) to middle Miocene (Galeotti et al., 2002). We suppose that this ~50 cm interval immediately below the tephra represents a mixing/reworking zone associated with the creation (by slumping or winnowing) of the unconformity, prior to the deposition of the Pliocene laminated tephra. Below this level, sediment reworking/mixing is much less apparent. The uppermost $^{87}\text{Sr}/^{86}\text{Sr}$, $\delta^{13}\text{C}$, and $\delta^{18}\text{O}$ values (yielding early Miocene ages) are from 71.63 mcd, 63 cm below the base of the tephra.

ISOTOPES AND THE OLIGOCENE/MIOCENE BOUNDARY

The Oligocene/Miocene boundary corresponds to the onset of C6Cn.2n according to

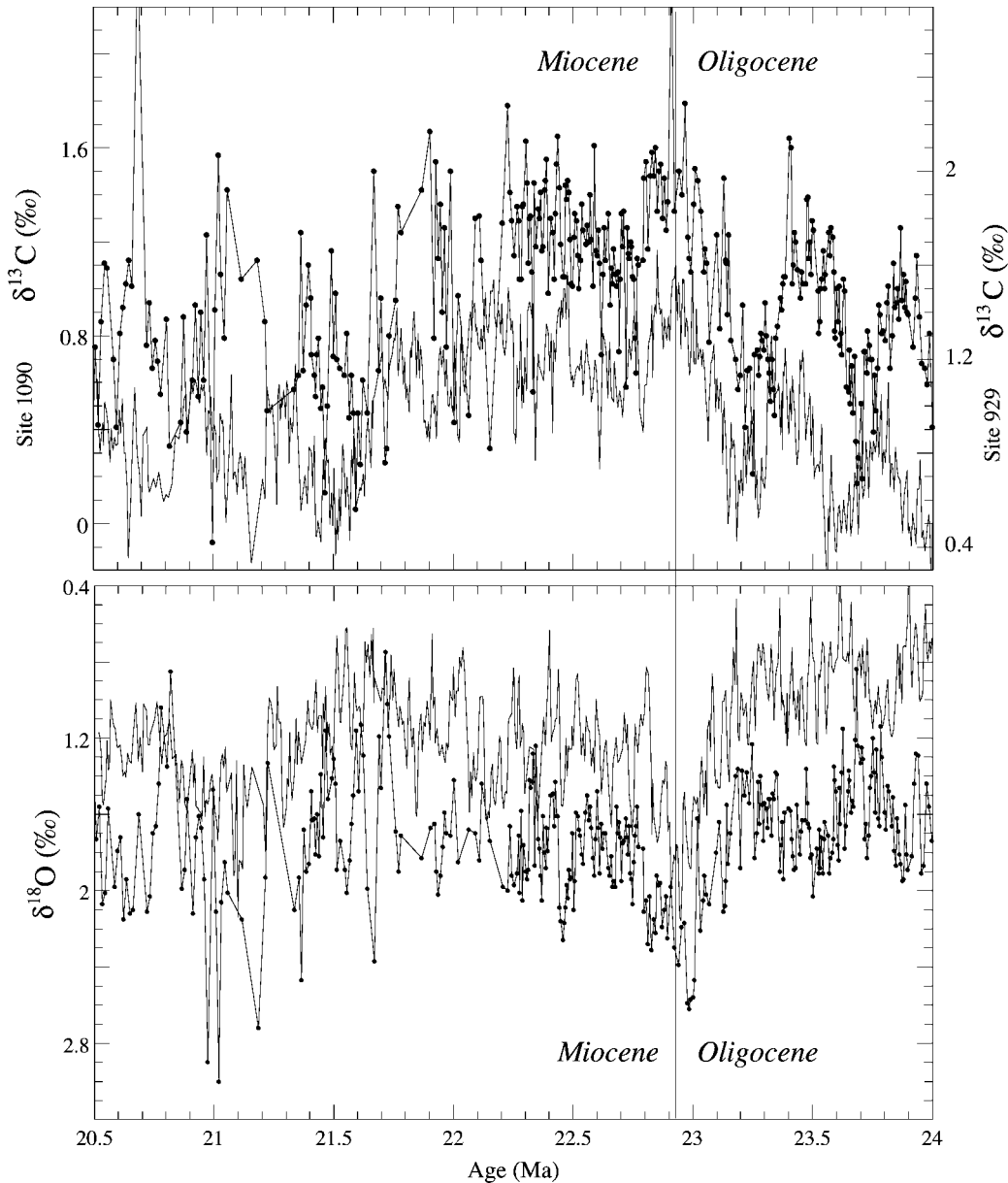


Figure 10. Site 1090 (lines with points) and Site 929 (lines without points) benthic $\delta^{13}\text{C}$ and $\delta^{18}\text{O}$ records (Flower et al., 1997; Zachos et al., 1997; Paul et al., 2000; Billups et al., 2002) placed on the astrochronological time scale (Shackleton et al., 1999) for Site 929 and the rescaled Cande and Kent (1992, 1995) time scale for Site 1090. The rescaling involved substituting the Oligocene/Miocene boundary age of Shackleton et al. (2000) into Cande and Kent's time scale.

the time scales of Berggren et al., (1995) and Cande and Kent (1992, 1995). At the Oligocene/Miocene boundary stratotype section in northern Italy at Lemme-Carrosio (Steininger et al., 1997), the primary magnetization component cannot be adequately resolved, and the magnetostratigraphy is difficult to interpret. Steininger et al. (1997) designated the 35 m level at Lemme-Carrosio as the stage boundary (based on biostratigraphy) and considered that the magnetostratigraphy indicates the onset of C6Cn.2n at this same level. Unfortu-

nately, the magnetostratigraphy at Lemme is too poor to be sure about this. The sphenoliths (*S. disbelemnos* and *S. delphix*) that are important for identifying the stage boundary at ODP Site 929 and DSDP Site 522 (Shackleton et al., 2000) and at Lemme-Carrosio (Steininger et al., 1997) are not present at Site 1090 (Marino and Flores, 2002b, 2002c).

ODP Site 929 (Ceara Rise, western equatorial Atlantic) yielded high-resolution isotope records spanning the Oligocene/Miocene boundary (Flower et al., 1997; Zachos et al.,

1997, 2001b; Paul et al., 2000). These benthic $\delta^{13}\text{C}$ and $\delta^{18}\text{O}$ isotope records were derived from the benthic foraminifer *Cibicidoides mundulus*. Shackleton et al. (1999) correlated the magnetic susceptibility records from ODP Sites 925, 926, 928, and 929 to an orbital template and, in so doing, produced an astrochronological age model that could be used to calibrate to the Site 929 isotope records. Unfortunately, none of the ODP Leg 154 sites yielded a magnetostratigraphy as the NRM was dominated by a drilling-induced rema-

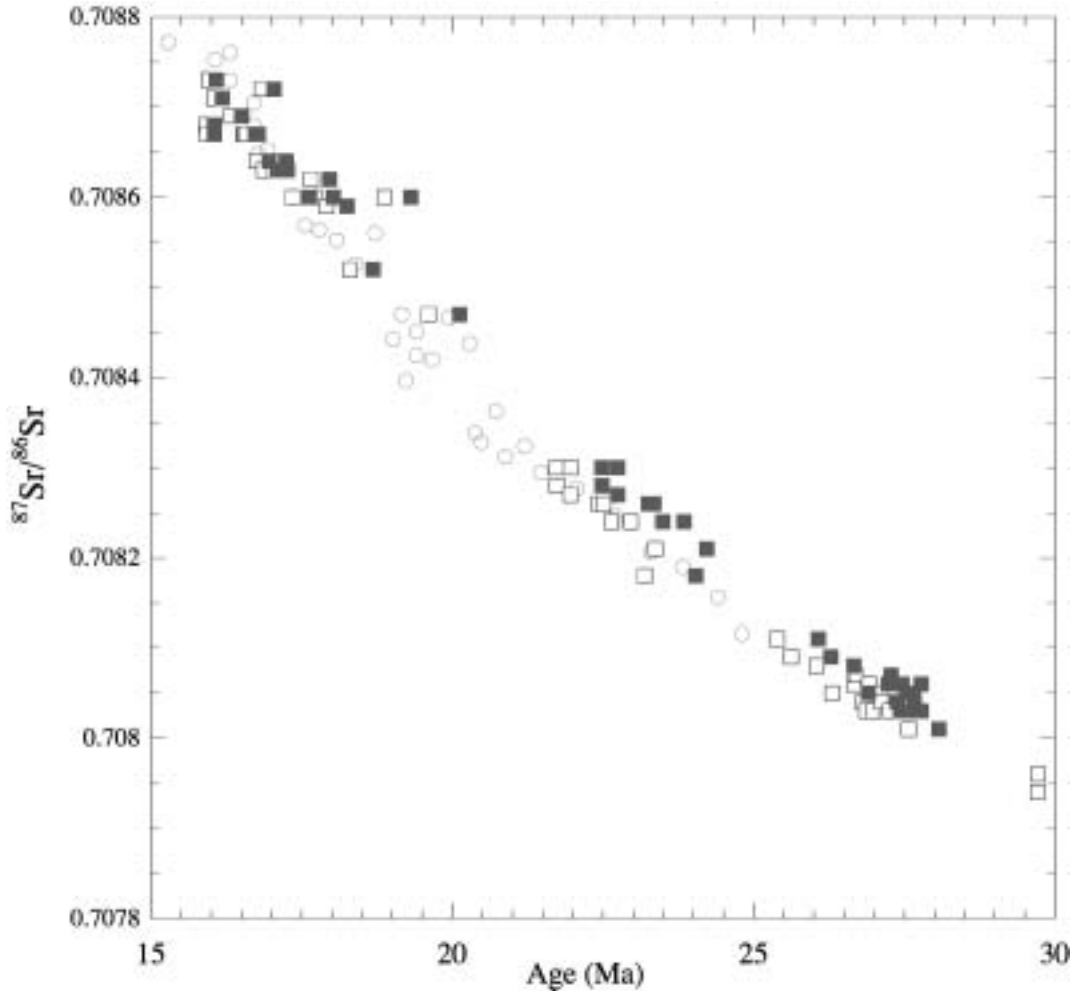


Figure 11. ODP Site 929 $^{87}\text{Sr}/^{86}\text{Sr}$ values (open circles) placed on the Site 929 astrochronology (Martin et al., 1999) compared with Site 1090 $^{87}\text{Sr}/^{86}\text{Sr}$ values placed on the Cande and Kent (1992, 1995) time scale (closed squares) and on the rescaled Cande and Kent (1992, 1995) time scale (open squares). The rescaling involved substituting the Oligocene/Miocene boundary age of Shackleton et al. (2000) into Cande and Kent's time scale.

nence (Shipboard Scientific Party, 1995). In order to transfer the Site 929 astrochronology to the geomagnetic polarity time scale, Shackleton et al. (2000) matched the biostratigraphic and isotope records from ODP Site 929 to DSDP Site 522, where polarity chrons close to the Oligocene/Miocene boundary can be recognized. By identification of C6Cn.2n at Site 522, and correlation of biostratigraphy and isotope stratigraphy from Site 522 to Site 929, Shackleton et al. (2000) used the Site 929 astrochronology to determine an age of 22.92 Ma for the onset of C6Cn.2n (the Oligocene/Miocene boundary). This age estimate is 880 k.y. younger than the age given by Cande and Kent (1992, 1995) (23.8 Ma) for this stage boundary.

The identification of subchrons within C6Cn at Site 522 is somewhat controversial. At Hole 522, C6Cn.2n as identified by Shack-

leton et al. (2000) was interpreted as C6Cn.1n by Tauxe and Hartl (1997). At Site 1090, the magnetostratigraphy can be unambiguously interpreted and therefore provides a means of testing the correlation of Shackleton et al. (2000). In Figure 10, we compare the Site 929 $\delta^{13}\text{C}$ and $\delta^{18}\text{O}$ records placed on their astrochronological time scale (Shackleton et al., 1999) with the Site 1090 record placed on a rescaled Cande and Kent (1992, 1995) time scale. The rescaling of the Cande and Kent (1992, 1995) time scale involved replacing their calibration point for the onset of C6Cn.2n (23.8 Ma), equivalent to the Oligocene/Miocene boundary, with the Shackleton et al. (2000) age for the same polarity chron/stage boundary (22.92 Ma). In this way, we follow Cande and Kent in using the assumption of smoothly varying South Atlantic seafloor spreading rates for interpolation to ad-

jacent absolute-age tie-points at 14.8 Ma (onset of C5ADr) and at 33.7 Ma for C13r (0.14). The resulting match of $\delta^{13}\text{C}$ and $\delta^{18}\text{O}$ records from Sites 929 and 1090 (Fig. 10) is convincing close to the Oligocene/Miocene boundary (22.92 Ma). Below the Oligocene/Miocene boundary, the Site 1090 record, particularly the $\delta^{13}\text{C}$ record, appears to become progressively older than the correlative features in the Site 929 record (Fig. 10). This finding indicates that a simple rescaling of Cande and Kent is insufficient to reconcile the two age models, although it does support the age for the Oligocene/Miocene boundary given by Shackleton et al. (2000).

In Figure 11, Site 929 $^{87}\text{Sr}/^{86}\text{Sr}$ data derived from planktic foraminifera and placed on the Site 929 astrochronological time scale (Martin et al., 1999) are compared with the Site 1090 $^{87}\text{Sr}/^{86}\text{Sr}$ data placed on the Cande and Kent

time scale and the rescaled Cande and Kent time scale just described. The rescaling results in enhanced correlation of the Site 929 and Site 1090 $^{87}\text{Sr}/^{86}\text{Sr}$ data sets for this time interval.

CONCLUSIONS

The magnetostratigraphy at ODP Site 1090 exhibits an almost complete record of polarity chrons C17r to C5Cn (38–16 Ma). The polarity-zone pattern fit to the GPTS appears unambiguous for the early Miocene and for most of the Oligocene and middle Eocene–late Eocene. There are, however, two options for the magnetostratigraphic interpretation in the vicinity of the Eocene/Oligocene boundary (Fig. 5). Option 1 is more consistent with the nanofossil biostratigraphy (Marino and Flores, 2002a), but option 2 is favored by the foraminiferal biostratigraphy (Galeotti et al., 2002) and by the fit of the polarity-zone pattern to the C13r–C13n–C12r “fingerprint” (Fig. 5). Strontium isotope stratigraphy is consistent with reference seawater $^{87}\text{Sr}/^{86}\text{Sr}$ curves for option 1, but not for option 2 (Fig. 6). Oxygen and carbon isotope data from benthic foraminifera compare favorably with the Cenozoic global composite for option 1 but not for option 2 (Fig. 7).

The option 1 interpretation of the polarity stratigraphy implies high sedimentation rates in the C13r and C13n polarity chrons, reaching 38 m/m.y. (Fig. 8). Sedimentation rates within polarity chrons varied by an order of magnitude from 4 to 38 m/m.y. with a hiatus in the early Oligocene affecting the C11n–C12r (29.5–32.8 Ma) interval and having a duration of ~3.3 m.y. (Figs. 5 and 8). C11n and C12r are only partially recorded due to this hiatus. Option 1 results in a normal-polarity zone in the 264–267 mcd interval (Fig. 4) within C13r (Fig. 5) that has not been previously recognized in a magnetostratigraphic section. Note that three “cryptochrons” appear in C13r in Cande and Kent (1992, 1995) (Fig. 5) on the basis of “tiny wiggles” in oceanic magnetic anomaly data. Bice and Montanari (1988) found one normal-polarity sample in the top third of C13r at Massignano, Italy, the Eocene/Oligocene boundary stratotype. Lowrie and Lanci (1994) resampled the Massignano section and concluded that there were no normal-polarity intervals within C13r. This conclusion appears to be corroborated by the study of cores recovered from a borehole drilled at Massignano (Lanci et al., 1996). The option 1 interpretation at Site 1090 yields a mean sedimentation rate within C13r of 38 m/m.y. (Fig. 8), more

than four times the sedimentation rate within C13r at Massignano. The high sedimentation rates in C13r at Site 1090 appear to have facilitated the recording of a short subchron (“cryptochron”) in the 264–267 mcd interval (Fig. 4). The 3-m-thick normal-polarity zone implies a duration for the C13r.1n subchron of 79 k.y., comparable with the duration of the Jaramillo Subchron.

Apart from the apparent subchron within C13r, two polarity subchrons not included in the Cande and Kent (1992, 1995) time scale are observed at Site 1090. One of these (C5Dr.1n) is well defined at Site 1090 (Figs. 3A and 5) and was included in versions of the GPTS prior to Cande and Kent, although it was relegated to cryptochron status by Cande and Kent. This normal-polarity subchron was identified in the North Pacific magnetic anomaly stack (Blakely, 1974). Another normal-polarity subchron (C7Ar.1n) recorded at Site 1090 (Figs. 3B and 5) has not been recognized in magnetostratigraphic or oceanic magnetic anomaly records. The reversal marking the onset of C7n.1r at 160.38 mcd and the unidentified normal-polarity zone within the hiatus at ~221 mcd (Fig. 3B) were used by Guyodo et al. (2002) as a test for u-channel deconvolution software, based on the protocol of Oda and Shibuya (1996).

The match of oxygen and carbon isotope records from Site 1090 to Site 929 (Ceara Rise) allows the Site 929 astrochronology (Shackleton et al., 1999) to be transferred to polarity zones at Site 1090 and hence to the GPTS. The result of the exercise is consistent with the age of the Oligocene/Miocene boundary (22.92 Ma) given by Shackleton et al. (2000). A simple rescaling of the Cande and Kent (1992, 1995) time scale incorporating the new Oligocene/Miocene boundary age does not, however, provide satisfactory correlation to the Site 929 chronology prior to the boundary interval (Fig. 10).

An outstanding dilemma at Site 1090 concerns the age of the 10 m of nanofossil ooze immediately below the unconformity at 71 mcd. The $^{87}\text{Sr}/^{86}\text{Sr}$, $\delta^{13}\text{C}$, $\delta^{18}\text{O}$, and paleomagnetic data all indicate a late early Miocene age, in spite of the presence of a foraminiferal species identified as *Globorotalia sphericomiozea* (Fig. 9) that is usually associated with the Messinian or early Pliocene.

ACKNOWLEDGMENTS

We thank Don McNeil and Ben Flower for insightful reviews of the manuscript. Silvia Iaccarino, Isabella Premoli-Silva, and Jim Kennett gave us their opinions on the identification of *Globorotalia sphericomiozea*. We thank Dave Hodell for his com-

ments and suggestions. We are indebted to the staff of the Ocean Drilling Program (ODP) for facilitating this study, and we particularly appreciate the assistance of the staff at the ODP Bremen Core Repository. Oxygen isotope studies were partially supported by a National Science Foundation (NSF) postdoctoral fellowship and by NSF grant OCE 0095976 (to Billups). Magnetostratigraphic and other studies of ODP Leg 177 sediments have been supported by a USSSP (United States Science Support Program) grant administered by the Ocean Drilling Program through Texas A&M University, and by the U.S. National Science Foundation (OCE-97-11424) (to Channell).

REFERENCES CITED

- Berggren, W.A., 1992, Paleogene planktonic foraminifer magnetostratigraphy of the southern Kerguelan Plateau (Site 747–749), in Wise, S.W., Jr., Schlich, R., et al., Proceedings of the Ocean Drilling Program, Scientific results, Volume 120: College Station, Texas, Ocean Drilling Program, p. 551–568.
- Berggren, W.A., Hamilton, N., Johnson, D.A., Pujol, C., Weiss, W., Cepek, P., and Gombos, A.M., Jr., 1983, Magnetostratigraphy of Deep Sea Drilling Project Leg 72, Sites 515–518, Rio Grande Rise (South Atlantic), in Barker, P.E., Carlson, R.L., Johnson, D.A., et al., Initial reports of the Deep Sea Drilling Project, Volume 72: Washington, D.C., Government Printing Office, p. 939–948.
- Berggren, W.A., Kent, D.V., Obradovich, J.D., and Swisher, C.C., III, 1992, Toward a revised Paleogene geochronology, in Prothero, D.R., and Berggren, W.A., eds., Eocene–Oligocene climatic and biotic evolution: Princeton, New Jersey, Princeton University Press, p. 29–45.
- Berggren, W.A., Kent, D.V., Swisher, C.C., and Aubry, M.P., 1995, A revised Cenozoic geochronology and chronostratigraphy in time scales and global stratigraphic correlations: A unified temporal framework for an historical geology, in Berggren, W.A., Kent, D.V., Aubry, M.-P., and Hardenbol, J., eds., Geochronology, time-scales, and stratigraphic correlation: SEPM (Society for Sedimentary Geology) Special Publication 54, p. 129–212.
- Bice, D.M., and Montanari, A., 1988, Magnetic stratigraphy of the Massignano section across the Eocene/Oligocene boundary in the Marche-Umbria basin (Italy), in Premoli-Silva, I., Coccioni, I., and Montanari, A., eds., The Eocene/Oligocene boundary in the Marche-Umbria basin (Italy): International Subcommission on Paleogene Stratigraphy, Special Publication II, v. 4, p. 111–117.
- Billups, K., Channell, J.E.T., and Zachos, J., 2002, Late Oligocene to early Miocene paleoceanography from the subantarctic South Atlantic (ODP Leg 177): Paleoceanography, v. 17, no. 1, 10.1029/2000PA000568.
- Blakely, R.J., 1974, Geomagnetic reversals and crustal spreading rates during the Miocene: Journal of Geophysical Research, v. 79, p. 2979–2985.
- Blow, W.H., 1969, Late middle Eocene to Recent planktonic foraminiferal biostratigraphy, in Brönniman, P., and Renz, H.H., eds., Proceedings of the First International Conference on Planktonic Microfossils, Geneva, 1967: Leiden, E.J. Brill, v. 1, p. 199–422.
- Bukry, D., 1973, Low-latitude coccolith biostratigraphic zonation, in Edgar, N.T., Saunders, J.B., et al., Initial reports of the Deep Sea Drilling Project, Volume 15: Washington, D.C., Government Printing Office, p. 685–703.
- Cande, S.C., and Kent, D.V., 1992, A new geomagnetic polarity timescale for the Late Cretaceous and Cenozoic: Journal of Geophysical Research, v. 97, p. 13,917–13,951.
- Cande, S.C., and Kent, D.V., 1995, A new geomagnetic polarity timescale for the Late Cretaceous and Cenozoic: Journal of Geophysical Research, v. 100, p. 6093–6095.

- Ciesielski, P.F., Kristoffersen, Y., et al., 1988, Proceedings of the Ocean Drilling Program, Initial Reports, Volume 114: College Station, Texas, Ocean Drilling Program, (CD-ROM; www-odp.tamu.edu/publications/114_SR).
- Clement, B.M., and Robinson, F., 1987, The magnetostratigraphy of Leg 94 sediments, in Ruddiman, W.F., Kidd, R.B., Thomas, E., et al., Initial reports of the Deep Sea Drilling Project, Volume 94: Washington, D.C., Government Printing Office, p. 635–650.
- Coccioni, R., Monaco, P., Monechi, S., Nocchi, M., and Parisi, G., 1988, Biostratigraphy of the Eocene-Oligocene boundary at Massignano (Ancona, Italy), in Premoli-Silva, I., Coccioni, R., and Montanari, A., eds., The Eocene-Oligocene boundary in the Umbria-Marche Basin (Italy): Ancona, International Union of Geological Sciences Special Publication: Ancona, Italy, Fratelli Annibelli Publishers, p. 59–74.
- Flower, B.P., Zachos, J.C., and Paul, H., 1997, Milankovitch-scale climate variability recorded near the Oligocene/Miocene boundary, in Shackleton, N.J., Curry, W.B., Richter, C., Bralower, T.J., et al., Proceedings of the Ocean Drilling Program, Scientific results, Volume 154: College Station, Texas, Ocean Drilling Program, p. 433–439.
- Fornaciari, E., Raffi, I., Rio, D., Villa, G., Backman, J., and Olfasson, G., 1990, Quantitative distribution patterns of Oligocene and Miocene calcareous nanofossils from the western equatorial Indian Ocean, in Duncan, R.A., Backman, J., Peterson, L.C., et al., Proceedings of the Ocean Drilling Program, Scientific results, Volume 115: College Station, Texas, Ocean Drilling Program, p. 237–254.
- Galeotti, S., Coccioni, R., and Gersonde, R., 2002, Middle Eocene–early Pliocene planktic foraminiferal biostratigraphy of ODP Leg 177, Site 1090, Agulhas Ridge: *Marine Micropaleontology*, v. 45, p. 357–381.
- Gersonde, R., Hodell, D.A., Blum, P., et al., 1999, Proceedings of the Ocean Drilling Program, Initial Reports, Volume 177: College Station, Texas, Ocean Drilling Program, (CD-ROM; www-odp.tamu.edu/publications/177_SR).
- Guyodo, Y., Channell, J.E.T., and Thomas, R., 2002, Deconvolution of u-channel paleomagnetic data near geomagnetic reversals and short events: *Geophysical Research Letters*, v. 29, 1845, doi: 10.1029/2002GL014963.
- Hailwood, E.A., and Clement, B., 1991a, Magnetostratigraphy of Sites 703 and 704, Meteor Rise, southeastern South Atlantic, in Ciesielski, P.F., Kristoffersen, Y., et al., Proceedings of the Ocean Drilling Program, Scientific results, Volume 114: College Station, Texas, Ocean Drilling Program, p. 367–386.
- Hailwood, E.A., and Clement, B., 1991b, Magnetostratigraphy of Sites 699 and 700, East Georgia Basin, in Ciesielski, P.F., Kristoffersen, Y., et al., Proceedings of the Ocean Drilling Program, Scientific results, Volume 114: College Station, Texas, Ocean Drilling Program, p. 337–357.
- Hodell, D.A., and Woodruff, F., 1994, Variations in the strontium isotopic ratio of seawater during the Miocene: Stratigraphic and geochemical implications: *Paleoceanography*, v. 9, p. 405–426.
- Hornibrook, B., Brazier, R.C., and Strong, C.P., 1989, Manual of New Zealand Permian to Pleistocene foraminiferal biostratigraphy: New Zealand Geological Survey Paleontological Bulletin, v. 56, p. 175 p.
- Inokuchi, H., and Heider, F., 1992, Magnetostratigraphy of sediments from Sites 748 and 750, Leg 120, in Wise, S.W., Jr., Schlich, R., et al., Proceedings of the Ocean Drilling Program, Scientific results, Volume 120: College Station, Texas, Ocean Drilling Program, p. 247–252.
- Jenkins, D.G., 1971, New Zealand Cenozoic planktonic foraminifera: New Zealand Geological Survey Paleontological Bulletin, v. 42, 278 p.
- Jenkins, D.G., 1975, Cenozoic planktonic foraminiferal biostratigraphy of the southwestern Pacific and Tasman Sea, in Kennett, J.P., Houtz, R.E., et al., Initial reports of the Deep Sea Drilling Project, Volume 29: Washington, D.C., Government Printing Office, p. 449–467.
- Jenkins, D.G., 1978, Neogene planktonic foraminifera from DSDP Leg 40 Sites 360 and 362 in the southeastern Atlantic, in Bolli, H.M., Ryan, W.B.F., Initial reports of the Deep Sea Drilling Project, Volume 40: Washington, D.C., Government Printing Office, p. 723–739.
- Jenkins, D.G., 1993, Cenozoic southern mid- and high-latitude biostratigraphy and chronostratigraphy based on planktonic foraminifera, in Kennett, J.P., and Warrke, D.A., eds., The Antarctic paleoenvironment: A perspective on global change: American Geophysical Union Antarctic Research Series, v. 60, p. 125–144.
- Keating, B., and Sakai, H., 1991, Magnetostratigraphic studies of sediments from Site 744, southern Kerguelen Plateau, in Wise, S.W., Jr., Schlich, R., et al., Proceedings of the Ocean Drilling Program, Scientific results, Volume 120: College Station, Texas, Ocean Drilling Program, p. 771–794.
- Kennett, J.P., and Srinivasan, M., 1983, Neogene planktonic foraminifera: A Phylogenetic Atlas: Stroudsburg, Pennsylvania, Hutchinson Ross Publishing Company, 265 p.
- Kirschvink, J.L., 1980, The least squares lines and plane analysis of paleomagnetic data: *Royal Astronomical Society Geophysical Journal*, v. 62, p. 699–718.
- Lanci, L., Lowrie, W., and Montanari, A., 1996, Magnetostratigraphy of the Eocene/Oligocene boundary in a short drill-core: *Earth and Planetary Science Letters*, v. 143, p. 37–48.
- Lowrie, W., and Lanci, L., 1994, Magnetostratigraphy of Eocene–Oligocene boundary sections in Italy: No evidence for short subchrons within chrons 12R and 13R: *Earth and Planetary Science Letters*, v. 126, p. 247–258.
- Lowrie, W., Alvarez, W., Napoleone, G., Perch-Nielsen, K., Premoli-Silva, I., and Toumarkine, M., 1982, Paleogene magnetic stratigraphy in Umbrian pelagic carbonate rocks: The Contessa sections, Gubbio: *Geological Society of America Bulletin*, v. 93, p. 414–432.
- Marino, M., and Flores, J.A., 2002a, Middle Eocene to early Oligocene calcareous nanofossil stratigraphy at Leg 177 Site 1090: *Marine Micropaleontology*, v. 45, p. 383–398.
- Marino, M., and Flores, J.A., 2002b, Miocene to Pliocene nanofossil biostratigraphy at ODP Leg 177 Sites 1088 and 1090: *Marine Micropaleontology*, v. 45, p. 291–307.
- Marino, M., and Flores, J.A., 2002c, Data report: Calcareous nanofossil stratigraphy at Sites 1088 and 1090 (ODP Leg 177, Southern Ocean), in Gersonde, R., Hodell, D.A., and Blum, P., Proceedings of the Ocean Drilling Program, Scientific results, Volume 177: College Station, Texas, Ocean Drilling Program (www.odp.tamu.edu/publications/177_SR).
- Martin, E.E., Shackleton, N.J., Zachos, J.C., and Flower, B.P., 1999, Orbitally-tuned Sr isotope chemostratigraphy for the late middle to late Miocene: *Paleoceanography*, v. 14, p. 74–83.
- Mead, G.A., and Hodell, D.A., 1995, Controls on the $^{87}\text{Sr}/^{86}\text{Sr}$ composition of seawater from the middle Eocene to Oligocene: Hole 689B, Maud Rise, Antarctica, *Paleoceanography*, v. 10, p. 327–346.
- Miller, K.G., Wright, J.D., and Fairbanks, R.G., 1991, Unlocking the ice house: Oligocene–Miocene oxygen isotopes, eustasy and margin erosion: *Journal of Geophysical Research*, v. 96, p. 6829–6848.
- Monechi, S., and Thierstein, H.R., 1985, Late Cretaceous–Eocene nanofossil and magnetostratigraphic correlations near Gubbio, Italy: *Marine Micropaleontology*, v. 9, p. 419–440.
- Nocchi, M., Parisi, G., Monaco, P., Monechi, S., Madile, M., Napoleone, G., Ripepe, M., Orlando, M., Premoli-Silva, I., and Bice, D.V., 1986, The Eocene-Oligocene boundary in the Umbrian pelagic sequences, in Pommerol, C., and Premoli-Silva, I., eds., Terminal Eocene events: New York, Elsevier, p. 25–40.
- Oda, H., and Shibuya, H., 1996, Deconvolution of long-core paleomagnetic data of Ocean Drilling Program by Akaike's Bayesian Information Criterion minimization: *Journal of Geophysical Research*, v. 101, p. 2815–2834.
- Paul, H.A., Zachos, J.C., Flower, B.P., and Tripathi, A., 2000, Orbitally induced climate and geochemical variability across the Oligocene/Miocene boundary: *Paleoceanography*, v. 15, p. 471–485.
- Pin, C., and Bassin, C., 1992, Evaluation of a Sr-specific extraction chromatographic method for isotopic analysis in geologic materials: *Analytica Chimica Acta*, v. 269, p. 249–255.
- Poore, R.Z., Tauxe, L., Percival S.F., Jr., LaBrecque, J.L., Wright, R., Petersen, N.P., Smith, C.C., Tucker, P., and Hsu, K.J., 1984, Late Cretaceous–Cenozoic magnetostratigraphy and biostratigraphic correlations of the South Atlantic Ocean, Deep Sea Drilling Project Leg 73, in Hsu, K.J., LaBrecque, J.L., et al., Initial reports of the Deep Sea Drilling Project, Volume 73: Washington, D.C., Government Printing Office, p. 645–655.
- Premoli-Silva, I., Orlando, M., Monechi, M., Madile, M., Napoleone, G., and Ripepe, M., 1988, Calcareous plankton biostratigraphy and magnetostratigraphy at the Eocene/Oligocene transition in the Gubbio area, in Premoli-Silva, I., Coccioni, R., Montanari, A., eds., The Eocene-Oligocene boundary in the Umbria-Marche Basin (Italy): Ancona, International Union of Geological Sciences Commission on Stratigraphy, International Subcommittee on Paleogene Stratigraphy Report, p. 137–161.
- Radford, S.S., and Li, Q., 1993, Eocene–Miocene high latitude biostratigraphy, in Hailwood, E.A., Kidd, R.B., eds., High resolution stratigraphy: Geological Society [London] Special Publication 70, p. 131–136.
- Salamy, K.A., and Zachos, J.C., 1999, Latest Eocene–early Oligocene climate change and Southern Ocean fertility: Inferences from sediment accumulation and stable isotope data: *Paleogeography, Paleoclimatology, Paleocology*, v. 145, p. 61–77.
- Scott, G.H., Bishop, S., and Burt, B.J., 1990, Guide to some Neogene globorotalids (Foraminifera) from New Zealand: New Zealand Geological Survey Paleontological Bulletin, v. 61, 135 p.
- Shackleton, N.J., 1974, Attainment of isotope equilibrium between ocean water and the benthonic foraminifera genus *Uvigerina*: Isotopic changes in the ocean during the last glacial: *Colloques Internationaux du Centre National de la Recherche Scientifique*, 219, p. 203–209.
- Shackleton, N.J., Crowhurst, S.J., Weedon, G., and Laskar, L., 1999, Astronomical calibration of Oligocene–Miocene time: *Royal Astronomical Society Geophysical Journal*, v. 357, p. 1909–1927.
- Shackleton, N.J., Hall, M.A., Raffi, I., Tauxe, L., and Zachos, J., 2000, Astronomical calibration age for the Oligocene–Miocene boundary: *Geology*, v. 28, p. 447–450.
- Shipboard Scientific Party, 1995, Site 926, in Curry, W.B., Shackleton, N.J., Richter, C., et al., Proceedings of the Ocean Drilling Program, Scientific results, Volume 154: College Station, Texas, Ocean Drilling Program, p. 153–232.
- Shipboard Scientific Party, 1999, Site 1090, in Gersonde, R., Hodell, D.A., Blum, P., et al., Proceedings of the Ocean Drilling Program, Scientific results, Volume 177: College Station, Texas, Ocean Drilling Program 77845–9547, p. 1–97.
- Spieß, V., 1990, Cenozoic magnetostratigraphy of Leg 113 drill sites, Maud Rise, Weddell Sea, Antarctica, in Barker, P.F., Kennett, J.P., et al., Proceedings of the Ocean Drilling Program, Scientific results, Volume 113: College Station, Texas, Ocean Drilling Program, p. 261–315.
- Steininger, F.F., Aubrey, M.P., Biolzi, M., Borsetti, A.M., Cati, F., Corfield, F., Gelati, R., Iaccarino, S., Napoleone, G., Rogli, F., Rotzel, R., Spezzaferri, S., Tateo, F., Villa, G., and Zevenboom, D., 1997, Proposal for the global stratotype section and point (GSSP) for the base of the Neogene (the Paleogene/Neogene boundary), in Montanari, A., et al., eds., Miocene stratigraphy: An integrated approach: Amsterdam, Elsevier, p. 125–147.
- Stott, L.D., and Kennett, J.P., 1990, Antarctic Paleogene planktonic foraminifer biostratigraphy: ODP Leg 113, Sites 689 and 690, in Barker, P.F., Kennett, J.P., et al., Proceedings of the Ocean Drilling Program, Scientific

EOCENE TO MIOCENE STRATIGRAPHY AT ODP SITE 1090

- results, Volume 113: College Station, Texas, Ocean Drilling Program, p. 549–569.
- Tauxe, L., and Hartl, P., 1997, 11 million years of Oligocene geomagnetic field behavior: *Geophysical Journal International*, v. 128, p. 217–229.
- Tauxe, L., Tucker, P., Peterson, N.P., and LaBrecque, J.L., 1983, The magnetostratigraphy of Leg 73 sediments: *Palaeogeography, Palaeoclimatology, Palaeoecology*, v. 42, p. 65–90.
- Tauxe, L., Tucker, P., Peterson, N.P., and LaBrecque, J.L., 1984, Magnetostratigraphy of Leg 73 sediments, in Hsu, K.J., LaBrecque, J.L., et al., Initial reports of the Deep Sea Drilling Project, Volume 73: Washington, D.C., Government Printing Office, p. 609–621.
- Tucholke, B.E., and Embley, R.W., 1984, Cenozoic regional erosion of the abyssal seafloor off South Africa, in Schlee, J.S., ed., *Interregional unconformities and hydrocarbon accumulation*: American Association of Petroleum Geologists Memoir 36, p. 145–164.
- Weeks, R., Laj, C., Endignoux, L., Fuller, M., Roberts, A., Manganne, R., Blanchard, E., and Goree, W., 1993, Improvements in long-core measurement techniques: Applications in palaeomagnetism and palaeoceanography: *Geophysical Journal International*, v. 114, p. 651–662.
- Wei, W., 1991, Middle Eocene–lower Miocene calcareous nannofossil magnetobiochronology of ODP Holes 699A and 703A in the subantarctic South Atlantic: *Marine Micropaleontology*, v. 18, p. 143–165.
- Wei, W., and Thierstein, H.R., 1991, Upper Cretaceous and Cenozoic calcareous nannofossils of the Kerguelen Plateau (southern Indian Ocean) and Prdyz Bay (East Antarctica), in Barron, J., Larsen, B., et al., *Proceedings of the Ocean Drilling Program, Scientific results, Volume 119*: College Station, Texas, Ocean Drilling Program, p. 467–493.
- Wei, W., and Wise, S.W., 1989, Paleogene calcareous nannofossil magnetobiochronology: Results from South Atlantic DSDP 516: *Marine Micropaleontology*, v. 14, p. 119–152.
- Wei, W., and Wise, S.W., 1990, Middle Eocene to Pleistocene calcareous nannofossils recovered by Ocean Drilling Program Leg 113 in the Weddell Sea, in Barker, P.F., Kennett, J.P., et al., *Proceedings of the Ocean Drilling Program, Scientific results, Volume 113*: College Station, Texas, Ocean Drilling Program, p. 639–666.
- Wei, W., Villa, G., and Wise, S.W., 1992, Paleocceanographic implications of the Eocene–Oligocene calcareous nannofossils from Site 711 and 748 in the Indian Ocean, in Wise, S.W., Jr., Schlich, R., et al., *Proceedings of the Ocean Drilling Program, Scientific results, Volume 120*: College Station, Texas, Ocean Drilling Program, p. 979–999.
- Zachos, J.C., Flower, B.P., and Paul, H.A., 1997, A high resolution chronology of orbitally paced climate oscillations across the Oligocene/Miocene boundary: *Nature*, v. 388, p. 567–570.
- Zachos, J.C., Pagani, M., Sloan, L., Thomas, E., and Billups, K., 2001a, Trends, rhythms, and aberrations in global climate 65 Ma to Present: *Science*, v. 292, p. 686–693.
- Zachos, J.C., Shackleton, N.J., Revenaugh, J.S., Palike, H., and Flower, B.P., 2001b, Climate response to orbital forcing across the Oligocene-Miocene boundary: *Science*, v. 292, p. 274–278.

MANUSCRIPT RECEIVED BY THE SOCIETY 11 OCTOBER 2002
 REVISED MANUSCRIPT RECEIVED
 MANUSCRIPT ACCEPTED 14 NOVEMBER 2002

Printed in the USA